Pharmaceutical Technology Division
Department of Pharmacy
Faculty of Science
University of Helsinki

Development of a Novel Multichamber Microscale Fluid Bed with *In-line* Near Infrared Spectroscopy and *Non-invasive* Electrostatic Measurement

by

Eetu Räsänen

Academic Dissertation

To be presented, with the permission of
the Faculty of Science of the University of Helsinki,
for public criticism in Auditorium 1 at Viikki Infocentre (Viikinkaari 11)
on June 18th, 2003, at 12 noon

Helsinki 2003

Supervisor: Professor Jouko Yliruusi
Division of Pharmaceutical Technology
Department of Pharmacy
University of Helsinki
Finland

Reviewers: Professor Raimo Hiltunen
Division of Pharmacognosy
Department of Pharmacy
University of Helsinki
Finland

Docent Leena Hellén
Naantalin Apteekki
Naantali
Finland

Opponent: Docent Pasi Merkku
Linnan Apteekki
Turku
Finland

ISBN 952-10-1035-5 (print)
ISBN 952-10-1036-3 (pdf, http://ethesis.helsinki.fi/)
ISSN 1239-9469

Yliopistopaino
Helsinki 2003
Finland

ABSTRACT

Räsänen, E., 2003. *Development of a Novel Multichamber Microscale Fluid Bed with In-line Near Infrared Spectroscopy and Non-invasive Electrostatic Measurement*

Dissertationes Biocentri Viikki Universitatis Helsingiensis 15/2003, pp. 45.

ISBN 952-10-1035-5 (print) ISBN 952-10-1036-3 (pdf) ISSN 1239-9469

Drug product development is a slow and expensive process. Despite the streamlining of lead compounds discovery, the related costs show a steady increase year upon year. Increasing costs and limited availability of new drug molecules have brought about a special need to determine process behaviour with smaller amounts of materials. Novel miniaturised techniques with precise monitor and control solutions are required to facilitate the understanding and the optimisation of the problematic unit operations related to drug development.

The aim of the present study was to develop a multichamber microscale fluid bed device with *in-line* NIR spectroscopy and with a *non-invasive* electrostatic measurement. The process variables affecting *in-line* NIR moisture measurement during wet granulation were evaluated, and further, the NIR spectroscopy was applied for studying processing-induced transformations (PITs) and *in-line* monitoring of fluid bed drying process. The developed microscale fluid bed and the electrostatic measurement was utilised for studying the process behaviour of pharmaceutical solids.

The rapid and flexible NIR spectroscopy is a promising tool for pharmaceutical process and quality control. The electrostatic measurement described may help to relieve the understanding of the complex charging behaviour of pharmaceutics. The studies established that the pressure difference over the bed was a useful parameter for monitoring the process behaviour in a precisely controlled fluid bed conditions. The developed multichamber microscale fluid bed set-up is a novel cost-effective approach for the preformulation studies of a new expensive and scarce drug candidate.

TABLE OF CONTENTS

TABLE OF CONTENTS I

ACKNOWLEDGEMENTS II

List of abbreviations III

List of original publications IV

1. INTRODUCTION 1

2. THEORY 3

2.1 Fluidisation 3
2.2 Process analysis 7
2.2.1 Near infrared spectroscopy 7
2.2.2 Electrostatics 10

3. AIMS OF THE STUDY 13

4. EXPERIMENTAL 14

4.1 Materials 14
4.2 Multichamber microscale fluid bed 14
4.2.1 In-line NIR moisture measurement 16
4.2.2 Non-invasive electrostatic measurement 17
4.3 Process conditions 18
4.4 Characterisation of materials 18
4.5 FT-NIR spectroscopy 19
4.6 X-ray diffraction 19
4.7 Differential scanning calorimetry 20

5. RESULTS AND DISCUSSION 21

5.1 Studying water-solid interactions using NIR spectroscopy 21
5.1.1 Evaluation of spectral factors 22
5.1.2 Determination of hydrate formation during wet granulation 24
5.1.3 In-line monitoring of fluid bed drying in microscale 25
5.2 Studies using A multichamber microscale fluid bed 28
5.2.1 Electrostatic measurements 28
5.2.2 Dehydration studies 30
5.2.3 Characterisation of fluidisation behaviour 32

6. CONCLUSIONS 36

REFERENCES 37

ACKNOWLEDGEMENTS

This study was carried out at the Pharmaceutical Technology Division, Department of Pharmacy, University of Helsinki, during the years 1999-2003.

I would like to express my warmest gratitude to my supervisor Professor Jouko Yliruusi. Without his experience and ideas, this work would not have been possible.

Docent Jukka Rantanen is acknowledged for his friendship and encouragement. His enthusiasm into the physical pharmacy has been admirable and extremely important during these years.

I am grateful to Professor Jukka-Pekka Mannermaa for his guidance and support during this project. I express my gratitude to Seppo Lehtonen (Ilmasäätö Oy), Janne Mäkinen (Ilmasäätö Oy), Esko Lauronen and Pekka Konttinen, who have helped to build up the experimental fluid bed set-up.

I am thankful to my co-author, Dr. Matti Murtomaa, Anna Jørgensen, Docent Milja Karjalainen and Professor Heikki Vuorela for successful collaboration. I am also grateful to the whole staff of the Pharmaceutical Technology Division, especially to Sari Airaksinen, Leena Christiansen, Niina Kivikero, Niklas Laitinen, Paulus Seitavuopio and Osmo Antikainen for their co-operation and friendship.

I would like to thank Professor Raimo Hiltunen and Docent Leena Hellén, the reviewers of this thesis, for their comments and suggestions made.

Markku Rajaniemi is gratefully acknowledged for his favourable attitude to my studies and to this project during my military service. Orion Pharma and Pharmia Oy are acknowledged for the loan of the FT-NIR instruments.

The co-operation with National Technology Agency, TEKES (Finland) has enabled this project and the studies made. The grant for finishing the doctoral dissertation from University of Helsinki is also gratefully acknowledged.

Finally, my deepest gratitude belongs to my dear family and friends, especially to my deceased mother, for unfailing encouragement and support. I am grateful to my beloved wife, Elina, for her loving support and patience during this work.

Helsinki, June 2003

List of abbreviations

API	Active pharmaceutical ingredient
AWA	Apparent water absorbance
DSC	Differential scanning calorimetry
EUFEPS	European Federation for Pharmaceutical Sciences
FT-NIR	Fourier transform near infrared
GAMP	Good Automated Manufacturing Practise
IT	Information technology
LLD	Laser light diffractometer
MCC	Microscrystalline cellulose
MMFD	Multichamber microscale fluid bed device
NIR	Near infrared
PIA	Particles in air
PITs	processing-induced transformations
PVP	polyvinylpyrrolidone
SD	Standard deviation
SMCC	Silicified microcrystalline cellulose
URS	User Requirements Specification
WAXS	Wide-angle X-ray scattering
XRD	X-ray diffraction

List of original publications

This thesis is based on the following original papers, which are referred to in the text by the Roman numerals I-IV.

I Rantanen, J., Räsänen, E., Mannermaa, J.-P. and Yliruusi, J., 2000. In-line moisture measurement during granulation with a four wavelength near infrared sensor: an evaluation of particle size and binder effects. *European Journal of Pharmaceutics and Biopharmaceutics* **50** 271-276.

II Räsänen, E., Rantanen, J., Jørgensen, A., Karjalainen, M., Paakkari, T. and Yliruusi, J., 2001. Novel identification of pseudopolymorphic changes of theophylline during wet granulation using near infrared spectroscopy. *Journal of Pharmaceutical Sciences* **90** 389-396.

III Murtomaa, M., Räsänen, E., Rantanen, J., Bailey, A., Laine, E., Mannermaa, J.-P. and Yliruusi, J., 2002. Electrostatic measurement on a miniaturized fluidized bed. *Journal of Electrostatics* **57** 91-106.

IV Räsänen, E., Rantanen, J., Mannermaa, J.-P., Yliruusi, J. and Vuorela, H. Dehydration studies using a novel multichamber microscale fluid bed dryer with in-line NIR measurement. *Journal of Pharmaceutical Sciences*. (Accepted).

V Räsänen, E., Rantanen, J., Mannermaa, J.-P. and Yliruusi, J. The characterization of fluidization behavior using a novel multichamber microscale fluid bed. *Journal of Pharmaceutical Sciences*. (Submitted).

1. INTRODUCTION

Despite the streamlining of lead compounds discovery over recent years, average development times for new drugs has remained quite unaltered (Smith, 2001). Accordingly, there is a concern about a bottleneck created by initial exploratory drug research. For instance, the European Federation for Pharmaceutical Sciences (EUFEPS) has established a project called, *New Safe Medicines Faster*, to speed up the slow and expensive drug development process (Bjerrum, 2002). Some of the main research topics for the faster development process are automated miniaturised systems, process measurement technologies and seamless scaling techniques (Table 1).

Table 1. Important research topics for faster drug development process (Bjerrum, 2002)

- Functional gene analysis
- Pathophysiological understanding of diseases for target prioritisation
- *In vivo* and *in vitro* disease models
- Expanded use of modelling tools for *in silico* testing
- Miniaturised fast screens with a robotic base
- Use of information technology (IT) solutions throughout the development process
- Pharmacogenetic profiling and population genetics
- Predictive biomedical markers and surrogate endpoints
- Drug and gene delivery systems
- Toolboxes containing predictive methods and seamless scaling techniques
- Pharmacometrics including non-invasive testing methods and sensor technologies
- Process-measurement technologies to allow rational manufacturing
- Science-based regulatory guidelines reflecting the latest scientific developments

The development process of a new drug candidate will concentrate more and more on the early stages of drug development. Producing an oral dosage form using small quantities of an expensive and scarce new drug candidate is the perennial problem

of the formulating (Rowe, 2000). At the early stages in the drug product development, each lot of active drug, excipient, and formulated blends would be characterised as fully as possible (Brittain *et al.*, 1991). Novel small-scale devices may improve the rationality of characterisation of the materials' process behaviour. Simultaneously performed studies (multi-unit devices) save time and ensure a higher quality of results, although the characterisation of process behaviour is difficult. Increasing numbers of experiments can bring the same kind of effectiveness to the preformulation stage as what the high-throughput screening techniques have done for drug discovery (Smith, 2002).

Inadequate process behaviour (*e.g.*, poor flowability) can cause serious problems in drug manufacture. To improve the composition of the formulation and the properties of the final product, characterisation and understanding of the process behaviour is important. To emphasise and to speed up the drug development and the preformulation stage, new miniaturised process technologies are required. Alkan *et al.*, (1988) have described a small-scale coating device that fluidised solid materials by controlled vibration of a mesh through which drying air is passed. Recently, small-scale equipment has been utilised in studying the compression behaviour or scalability of the high-shear granulation process (Hancock *et al.*, 2000; Bock and Kraas, 2001). The results illustrate the fact that if we do not understand simplified small-scale phenomena, we will not have tools for systematic scaling-up studies or process optimisation in drug development.

Fluid beds are widely utilised in petroleum, metallurgical, agricultural and chemical industries (Davidson *et al.*, 1985). In pharmaceutical industry, fluid bed systems are mainly applied in coating, conveying, drying and granulation processes. Despite the great interest and the numbers of studies, pharmaceutical applications of fluid beds seem still to rely more or less on user experience than on the knowledge of the basic phenomena of the processes. Problems concerning the fluid beds have been the utilisation of the process analytical solutions, inadequate process control and complexity of the systems (*e.g.*, fluid bed granulators). Simplified, precisely monitored and controlled small-scale systems may allow novel tools for understanding, *e.g.*, the physicochemical background of the almost chaotic fluid bed processes of pharmaceutical materials.

2. THEORY

2.1 Fluidisation

When passing a gas through a bed of solid particles at a low velocity, the gas fluid first percolates through the void spaces between the particles. This stage is called the fixed bed (Fig. 1A). When the velocity of the gas is increased, particles begin to vibrate and the pressure drop across the bed increases. This is the expanded bed and at this stage, the bed performance is quite similar to that of the fixed bed. Insignificant increase in void fraction in the bed will be observed. At a certain velocity, the buoyancy of upward moving gas counterbalances the weight of the bed (interparticle forces denied). This stage is referred to as a bed at minimum fluidisation or an incipiently fluidised bed (Fig. 1B). The bed commences to behave like a dense fluid. At this point, the pressure drop across the bed equals the weight of the bed (Eq. 1),

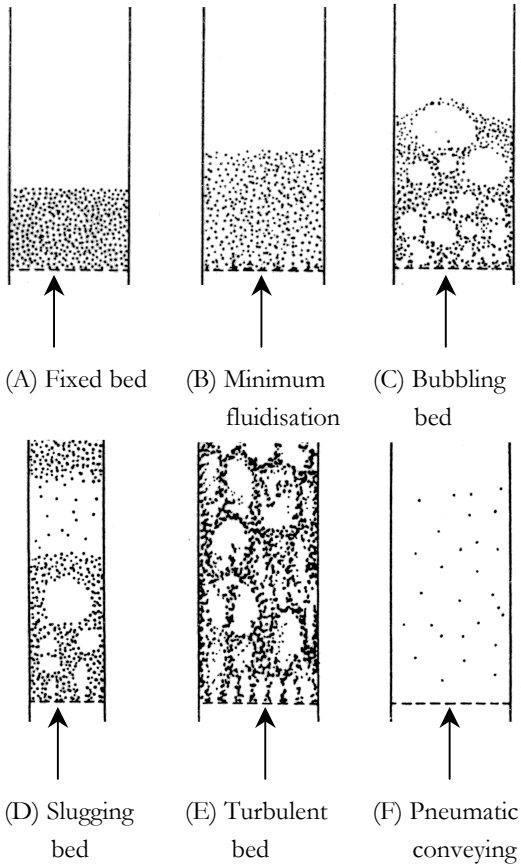

Figure 1. Various kinds of contacting of a batch of solids by gas (Kunii and Levenspiel, 1991).

$$\frac{\Delta p_b}{L_{mf}} = (1-\varepsilon_{mf})(\rho_s - \rho_g)g \qquad (1)$$

where Δp_b is the pressure drop across the bed (Pa), L_{mf} is the height of the bed at the minimum fluidisation (m), ε_{mf} is the void fraction in the bed at the minimum fluidising conditions, ρ_s, ρ_g are the densities of solid and gas (kg/m^3), and g is the acceleration of gravity, respectively (9.81 m^2/s). After the bed has been fluidised and the velocity of the air increases, the pressure drop across the bed stays constant but the height of the bed continues to increase (Fig. 1). The behaviour of the bed is highly dependent on the properties of solid materials and the velocity of the inlet gas.

The Eq.1, which has been experimentally verified numerous times, constitutes the fundamental fluidisation condition (Davidson *et al.*, 1985; Kunii and Levenspiel, 1991). At the minimum fluidisation, the bed may as well be considered both fixed and fluidised. Ergun (1952) has correlated experimental data (the Ergun equation) for pressure drops using different solids in packed beds

$$\frac{\Delta p_b}{L_{mf}} = 150\frac{(1-\varepsilon_m)^2}{\varepsilon_m{}^3}\frac{\mu u_0}{(\phi_s d_p)^2} + 1.75\frac{1-\varepsilon_m}{\varepsilon_m{}^3}\frac{\rho_g u_0{}^2}{\phi_s d_p} \quad (2)$$

where ε_m is the void fraction in a fixed bed, μ is the viscosity of a gas (kg/ms), u_0 is the superficial gas velocity (measured on the basis of an empty chamber) (m/s), ϕ_s is the sphericity of a particle (ratio of the surface area of a sphere of equal volume to the particle surface area), and d_p is the mean particle diameter (m). The first term in the left side is the viscous term, and the second term is the kinetic term.

A minimum fluidisation velocity (u_{mf}) represents the point of transition between the fixed and the fluidised states. The Eq. 2 and 3 can be applied to predict the u_{mf}. The u_{mf} (Eq. 3) can be found by combining Eqs. 1 and 2:

$$\frac{1.75}{\varepsilon_{mf}{}^3\phi_s}\left(\frac{d_p u_{mf}\rho_g}{\mu}\right)^2 + \frac{150(1-\varepsilon_{mf})}{\varepsilon_{mf}{}^3\phi_s{}^2}\left(\frac{d_p u_{mf}\rho_g}{\mu}\right) = \frac{d_p{}^3\rho_g(\rho_s-\rho_g)g}{\mu^2} \quad (3)$$

Eq. (3) is simplified by using dimensionless groups, $\mathrm{Re}_{p,mf}$ (Reynold's number for a particle in fluid at minimum fluidising condition) and Ar (Archimedes number). Simplified equation is written as

$$\frac{1.75}{\varepsilon_{mf}{}^3\phi_s}\mathrm{Re}_{p,mf}{}^2 + \frac{150(1-\varepsilon_{mf})}{\varepsilon_{mf}{}^3\phi_s{}^2}\mathrm{Re}_{p,mf} = Ar \quad (4)$$

where $\mathrm{Re}_{p,mf} = \left(\frac{d_p u_{mf}\rho_g}{\mu}\right)$, and $Ar = \frac{d_p^3\rho_g(\rho_s-\rho_g)g}{\mu^2}$. Further, when particle sphericity (ϕ_s) and void fraction of the bed (ε_{mf}) are difficult to determine or not available, the Eq. (3) can be rewritten as follows

$$K_1\mathrm{Re}_{p,mf}{}^2 + K_2\mathrm{Re}_{p,mf} = Ar \quad (5)$$

where $K_1 = \frac{1.75}{\varepsilon_{mf}^{\ 3}\phi_s}$, and $K_2 = \frac{150(1-\varepsilon_{mf})}{\varepsilon_{mf}^{\ 3}\phi_s^{\ 2}}$. It has been noticed those terms, K_1 and K_2, stay nearly constant over a wide range of different particles ($0.001 < \mathrm{Re}_{p,mf} < 4000$) (Wen and Yu, 1966). Eq. (5) may be solved, giving

$$\mathrm{Re}_{p,mf} = \sqrt{\left(\frac{K_1}{2K_2}\right)^2 + \frac{1}{K_2}Ar} - \frac{K_1}{2K_2} \tag{6}$$

for which terms $\frac{K_1}{2K_2}$ and $\frac{1}{K_2}$ has been published to various systems (Table 2).

Table 2. Values for constants in Eq. (6)

Definition of particles	$K_1/2K_2$	$1/K_2$	Reference
284 data points from literature	33.7	0.0408	Wen and Yu, 1966
Dolomite	25.3	0.0571	Saxena and Vogel, 1977
Coal, char and sphere	28.7	0.0494	Chitester *et al.*, 1984

For design and scaling-up purposes, it is important to be able to calculate the value of u_{mf} precisely and thus avoid a large number of experiments. Several authors have published their own detailed models for predicting the u_{mf} in different conditions (Wen and Yu, 1966; Saxena and Vogel, 1977; Chitester *et al.*, 1984; Noda *et al.*, 1986; Lippens and Mulder, 1993; Rao and Bheemarasetti, 2001). On the basis of the derivation above, the computational u_{mf} can be estimated

$$u_{mf} = \frac{\mu}{d_p\rho_g}\left(\sqrt{\left(\frac{K_2}{2K_1}\right)^2 + \frac{1}{K_1}Ar} - \frac{K_2}{2K_1}\right). \tag{7}$$

Methods have been proposed for predicting the mode of fluidisation. Geldart (1973) focused on the physical properties of the particle and created a model that is very common. This classification consists of four clearly recognisable groups, characterised by density differences between solid and gas (ρ_s-ρ_g) and mean particle size (Fig. 2). Between the groups, different fluidisation behaviour has been observed over a large range of the fluidisation velocity (Fig. 3). In addition, each flow regime has been established to have

their own distinctive density-height profile (Kunii and Levenspiel, 1991). The groups, defined by particle size, are as follows:

1. Group C, cohesive and very fine particles. Interparticle forces in this group are stronger than those resulting from the gas flow.

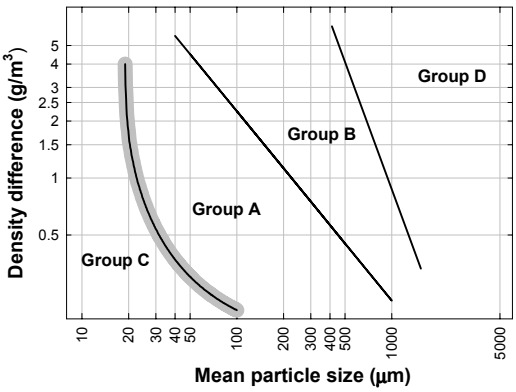

Figure 2. Geldart (1973) classification.

2. Group A, aeratable materials. The beds of powders in this group expand considerably before bubbling commences, and these solids fluidise easily.

3. Group B, sand-like solids. These solids fluidise well with vigorous bubbling action. The beds of powders expand only a little before bubbling starts (slightly above u_{mf}). The formed bubbles are small and they coalesce as they rise through the bed.

4. Group D, large and/or dense particles. Deep beds of these solids are difficult to fluidise and an enormous amount of gas is needed to fluidisation. The gas velocity in the dense phase is high and mixing of the solids relatively poor. Bubbles in the bed coalesce rapidly and grow to a large size. The bed of these solids spouts easily.

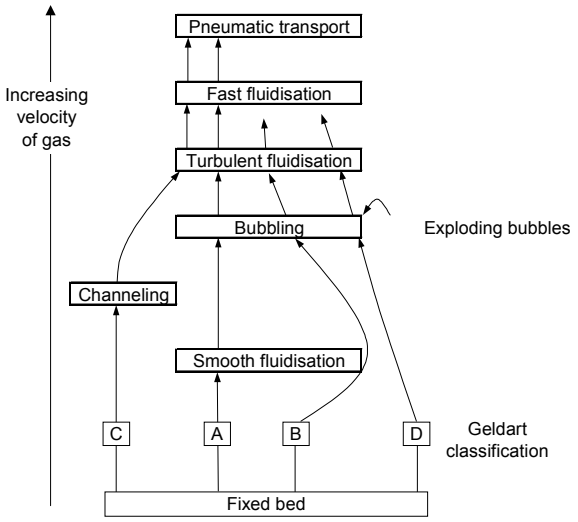

Figure 3. Fluidisation behaviour on the basis of the Geldart classification (Kunii and Levenspiel, 1991).

Between Geldart A and C solids there is an uncertain region of particles which have properties from both groups (Fig. 2). These particles flow well when fluidised (type A behaviour), but they block horizontal pipes (type C behaviour). An AC classification has been proposed for these solids.

2.2 Process analysis

To optimise pharmaceutical unit operations and to improve the quality of the final product, robust and reliable process control and monitoring solutions are necessary. Precisely controlled systems provide highly repeatable procedures that are essential to the drug product development (Browne and Olsson, 1998). Concerning process analytical chemistry, some views of the commonly used terms, *off-line*, *at-line*, *on-line*, *in-line* and *non-invasive* are defined (Callis *et al.*, 1987; Hassel and Bowman, 1998). The fundamental differences of these classes are that *off-line*, *at-line* and *on-line* solutions require sampling or sample transfer to analysers. In proportion, *in-line* measurement is done directly inside the process line and *non-invasive* measurement requires no physical sample contact. The two following sections describe some general aspects of utilised process analysis techniques.

2.2.1 Near infrared spectroscopy

The region of near infrared (NIR) spectroscopy lies between visible area and infrared region, respectively from 750 nm to 2600 nm. The measurement technique is fast and non-destructive, and therefore NIR spectroscopy has numerous applications in several industries (Williams and Norris, 1987; Osborne *et al.*, 1993; Workman, 1993; Blanco *et al.*, 1998, Workman 1999). In pharmaceutics, NIR spectroscopy has been utilised in, *e.g.*, the determination of degradation products (Drennen and Lodder, 1990) and an active pharmaceutical ingredient (API) of tablets (Gottfries *et al.*, 1993; Dreassi *et al.*, 1996; Han and Faulkner, 1996; Dyrby *et al.*, 2002; Laasonen *et al.*, 2003), the determination of polymorphic changes of API or excipient (Aldridge *et al.*, 1996; Buckton *et al.*, 1998; Jørgensen, 2002), the determination of particle size (Ciurzak *et al.*, 1986; Frake *et al.*, 1998; O'neil *et al.*, 1998; Rantanen and Yliruusi, 1998; O'neil *et al.*, 1999), and the monitoring of film coating (Kirsch and Drennen, 1996; Andersson *et al.*, 2000) and blending processes (Hailey *et al.*, 1996; Plugge and van der Vlies, 1996; Sekulic *et al.*, 1996).

When molecules are irradiated with an external source of energy they are exposed to energy changes. The incident beam of light (I_R) can be stated as a sum of transmitted light (T), reflected light (R) and absorbed light (A)

$$I_R = T + R + A. \quad (8)$$

In reflectance mode, the reflected radiation (R) can be stated

$$R = \frac{I}{I_0} \quad (9)$$

where I is the intensity of incident radiation and I_0 is the intensity of standard radiation.

The molecules can absorb photons that are of energy coincident with the characteristic vibrations of the molecule. The absorption leads to the excitation of the molecule to a higher energy level. Due to the method of measurement, the determination of actual absorbance is not possible. However, the apparent absorbance (A) can be calculated on the basis of R

$$A = \log\left(\frac{1}{R}\right) = \log\left(\frac{I_0}{I}\right). \quad (10)$$

All molecules and parts of molecules vibrate at their characteristic wavelength. Typically, the apparent absorbance is stated as a function of wavelength (λ, nm) or wave number (ν, cm^{-1})

$$\lambda = \frac{c}{f} \quad (11)$$

$$\upsilon = \frac{1}{\lambda} \quad (12)$$

where c is the velocity of light in a vacuum and f is the frequency in cycles per second (Hz).

Only vibrations that result in rhythmic changes in the dipole moment of a molecule can cause absorbencies in the infrared (Williams and Norris, 1987). In the NIR region, the absorption bands are mainly caused by overtones and combination vibrations of CH, NH, SH and OH groups (Osborne *et al.*, 1993). The fundamental absorption bands are in the mid IR region.

The vibration may be described as either stretching or bending (Pimental and McClellan, 1960). Stretching is movement along the axes of bonds, so that the distance between atoms changes (Fig. 4AB). Bending vibration involves the changes in the bond

angles between atoms (Fig. 4C-F). Both of these vibration modes give rise to overtone or combination bands that are observable in the NIR region.

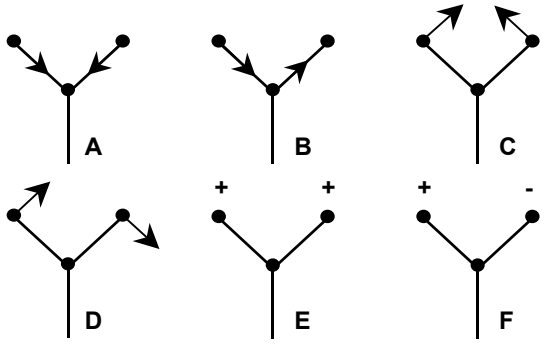

Figure 4. The modes of vibration in the case of a triatomic molecule or group AX_2. A) Symmetrical stretching B) Asymmetrical stretching C) Symmetrical in-plane bending (scissoring) D) Asymmetrical in-plane bending (rocking) E) Symmetrical out-of-plane bending (wagging) F) Asymmetrical out-of-plane bending (twisting) (Osborne *et al.*, 1993).

Numerous factors, *e.g.*, texture of the particle surface, the particle size and shape distributions, temperature and density of the sample have an effect on the back-reflected light and thereby the NIR measurement (Williams and Norris, 1987). When particle size increases, the scattering of the light diminishes and the light penetrates deeper into the material (Osborne *et al.*, 1993). The apparent absorbance (Eq. 10) increases. Norris and Williams (1983) studied ground wheat samples with varying mean particle sizes and found that the normalisation of spectral data effectively removed the particle size effect. Thereafter, various procedures have been suggested for modelling the particle size data from the NIR data (Ciurczak *et al.*, 1986; Ilari *et al.*, 1988; Frake *et al.*, 1997; O'Neil *et al.*, 1998; Rantanen and Yliruusi, 1998; O'Neil *et al.*, 1999).

One of the first pharmaceutical applications of NIR spectroscopy was the measurement of water (Stein and Ambrose, 1963; Sinsheimer and Poswalk, 1968). The absorption bands of pure water molecules (OH vibrations) occur at 760 nm, 970 nm, 1190 nm, 1450 nm and 1940 nm (Curcio and Petty, 1951; Buijs and Choppin, 1963, Osborne *et al.*, 1993). The most intense absorption bands are located at around 1450 nm (issued from the first overtone OH stretching vibrations) and 1940 nm (caused by a combination of OH stretching and bending vibrations). The absorption bands are the distributions of vibrations of different OH groups with varying energy levels (Buijs and Choppin, 1963; Fornes and Chaussidon, 1978; Maeda *et al.*, 1995). The dependency of the states of water molecules on their hydrogen bonding ability has been established (Luck, 1976). Using spectral treatment, the individual absorption maxima of each energy level can be distinguished and the NIR measurement can be applied for studying the

water-solid interactions within various materials (Iwamoto *et al.*, 1987; Delwiche *et al.*, 1991; Buckton *et al.*, 1998; Jørgensen *et al.*, 2002).

Water molecules can associate with solids in different ways (Zografi, 1988). In drug development, there is a special need to determine the interactions of water during processing. One of the most important reasons for this is the fact that the interactions can ultimately result in variations in the bioavailability of drugs (Haleblian and McCrone, 1969). Using the NIR spectroscopy, the determination of moisture in freeze dried product (Kamat *et al.*, 1989; Last and Prebble, 1993; Jones *et al.*, 1993; Derksen *et al.*, 1998) and the *on-line* moisture determination of microwave vacuum drier (White, 1994), the *at-line* determination of moisture content of gelatine capsules (Buice *et al.*, 1995; Berntsson *et al.*, 1997) and *in-situ* moisture determination of a cytotoxic compound during process optimisation (Hicks *et al.*, 2003) has been described. However, the first pharmaceutical process analytical applications of the NIR spectroscopy have been the monitoring of complex wet granulation (Watano *et al.*, 1990; White, 1994; Han and Faulkner, 1996; List and Steffens 1996; Frake *et al.*, 1997; Goebel and Steffens, 1998; Rantanen and Yliruusi, 1998; Rantanen *et al.*, 1998; Morris *et al.*, 2000). The effects of granulation on the structure of cellulose have also been studied (Buckton *et al.*, 1999). Recently, the NIR spectroscopy has been considered as such a promising method for pharmaceutical purposes that the pharmacopoeias have defined some characteristics of the analysis (Ph. Eur. 4th Ed., 2002; USP 26-NF 21, 2003).

2.2.2 Electrostatics

Electrostatic charging can be a serious problem (reduced process efficiency, explosions or fires) during drug product development (Hearn, 1998). Typically, the problems of the pharmaceutical materials are tried to be solves by way of modification of particle size or shape distributions, composition design, earth connection, humidifying or modifying process conditions (Staniforth *et al.*, 1989; Staniforth, 2000). However, the complete understanding of charging behaviour during processes is still lacking, and the solutions to the problems have been more or less unsatisfactory.

Electric charges are generated when electrons are transferred from one body to another. Typical situation is when two different materials are brought into contact and then separated (Harper, 1967). If one of the materials is an insulator (high resistivity),

there remains a net positive charge on one body and a net negative charge on the other. The sign and the amount of the charge depends on many factors such as particle size and shape (Carter *et al.*, 1998), nature and work functions (Bailey 1984), impurities (Eilbeck *et al.*, 1999; Eilbeck *et al.*, 2000; Murtomaa *et al.*, 2002a), amorphicity (Murtomaa *et al.*, 2002b), surface roughness (Vladykina *et al.*, 1985), relative humidity (Mackin *et al.*, 1993) and the energy of the contact (Cross, 1987).

The electrostatic force is directed along the line joining the particles and it is spherically symmetric. A vector form of Coulomb's law indicates the electrostatic force vector ($\overline{F}$) between two point charges,

$$\overline{F} = \frac{1}{4\pi\varepsilon_0}\frac{q_1 q_2}{r^2}\bar{u} = k\frac{q_1 q_2}{r^2}\bar{u} \tag{13}$$

where ε_0 is the permittivity of vacuum ($8.854 \cdot 10^{-12}$ C^2/Nm^2), q_1 and q_2 are the fixed charges, r is the separation distance of the points, $\bar{u}$ is the unit vector that has its origin at the "source of the force", k is the constant ($8.988 \cdot 10^9$ Nm^2/C^2). Coulomb's law assumed the charges to be at rest due to the fact that the charges in motion produce and experience magnetic forces. In addition, the expression is valid only for point charges.

For the charged bodies of arbitrary shape, there is no well-defined value of the separation distance. Generally, the electric field strength ($\overline{E}$) due to the continuous distribution of the charge can be found by integrating over the charge distribution

$$\overline{E} = k\int\frac{dq}{r^2}\bar{u} \tag{14}$$

where dq is the infinitesimal elements of charge. However, the integration required may sometimes be complex. Gauss's law states the net flux through a closed surface to the net charge (Q) enclosed by the surface

$$\oint \overline{E}\cdot dA = \frac{Q}{\varepsilon_0} \tag{15}$$

where A is the area of a surface. When the charge distribution has sufficient symmetry, Gauss's law can provide an elegant way to determine the electrostatic field in simple steps.

Under static conditions, the net (external-internal) field inside the conductor is zero. By Gauss's law, it can be inferred that any net charge on a conductor in an

electrostatic equilibrium resides on the surface (Fig. 5A). When an external electric field is applied to a conductor, free electrons of the conductor move very quickly in a direction opposite to the electric field. They leave unbalanced positive charges on the other side. The redistribution of the charge creates an internal electric field, which is in the opposite direction to the external field. The internal field will increase until the net field is zero.

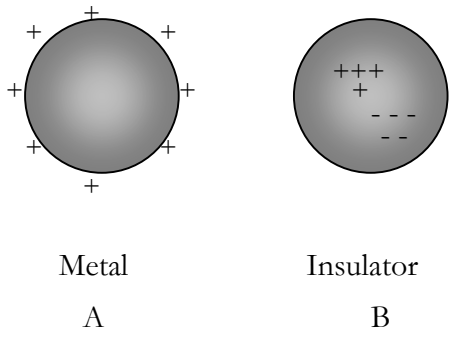

Figure 5. A) Any net charge placed on a metal sphere spreads very quickly over its surface. B) Net charges may be found in small region on the surface of an insulator.

Most of the pharmaceutical materials have relatively high resistivities, which prevent or retard the generated charge leaking away. (Fodor *et al.*, 1991; Bailey 1993; Grosvenor and Staniforth, 1996). The mobility of the electrons is restricted and local net charges regions can be found (Fig. 5B). In such materials, the redistribution of the electrons under an external electric field is also limited.

On the surface of the insulators, the sign and the amount of the charge can vary significantly. In order to transfer the charges away from the insulator, one has to contact the insulator at many points. In an ionised gas, both positive and negative charges move with the ions. One approach to increase the amount of free charge carriers is to increase the amount of water molecules in the current conditions. The phenomena have been studied using a cyclone apparatus, where the charge of a pharmaceutical excipient was decreased when the relative humidity in the apparatus was increased (Eilbeck *et al.*, 2000).

With pharmaceutics, electrostatic charging is a complex and particularly disturbing process. The charging can be generated during manufacturing or even during the use of drugs (inhalers). The local charges and long relaxation times of insulating materials increase the problems. On the subject of fluidisation, the electrostatic charging phenomenon is very complex. Interactions where the charges can be generated are several; particle-particle, particle-wall (triboelectric) and particle-gas interactions. Due to the fact that the fundamental theories are inadequate in describing and predicting the charging behaviour during processing, experimental knowledge of the behaviour of pharmaceutics in the controlled and monitored fluid bed conditions is required.

3. AIMS OF THE STUDY

Traditionally, pharmaceutical fluid beds have been studied with materials weighing from hundreds of grams to several kilograms. The fact that the availability of new and expensive drug candidates is often limited to few grams sets special demands for formulation and process optimisation. The aim of the present study was to develop an automated and instrumented *gram-scale* fluid bed set-up for the pharmaceutical preformulation. The specific aims of the study were:

1. to study the significance of particle size and binder effects for *in-line* NIR moisture measurement
2. to study the processing-induced transformations (PITs) of an active pharmaceutical ingredient (API) using FT-NIR spectroscopy and *in-line* NIR moisture measurement
3. to develop a *non-invasive* method for studying the charging behaviour of the pharmaceutical solids in a microscale fluid bed
4. to study the dehydration behaviour of model compounds using a developed multichamber microscale fluid bed
5. to characterise the fluidisation behaviour of model particles and pharmaceutical excipients using the multichamber microscale fluid bed.

4. EXPERIMENTAL

4.1 Materials

Studied excipients were lactose monohydrate (Pharmatose 80M, DMV Int., Veghel, the Netherlands) (III), microcrystalline cellulose (Avicel PH200 (III), PH 101 and PH 102 (V), FMC Int., Ireland), silicified microcrystalline cellulose (Prosolv 50 and 90, Penwest Pharmaceutical Co., Nastola, Finland) (V). The granulated materials were microcrystalline cellulose (Emcocel 50M, Penwest Pharmaceuticals, Nastola, Finland) (I) and anhydrous theophylline (theophyllinum anhydricum 200M, BASF, Ludwigshafen, Germany) (II, IV). Anhydrous theophylline was granulated using a planetary mixer (Kenwood KM400, Kenwood Ltd., UK). The batch size was 300 g of anhydrous theophylline, and different amounts of purified water were added. Theophylline monohydrate was prepared (II) by dissolving anhydrous theophylline in distilled water at 60 °C. The saturated solution was slowly cooled and the needle-like theophylline monohydrate was filtered by vacuum. Theophylline monohydrate was dried at room temperature until the moisture content was around 9 %.

The binders studied were polyvinylpyrrolidone (PVP) (Plasdone K-25, ISP Technologies Inc., Wayne, NJ, USA) (I), gelatin (Orion Pharma, Finland) (I) and purified water (II,IV). Solutions on purified water were prepared using 10 and 20% w/w of PVP (I). Glass beads (Jencons Ltd., Bedfordshire, England) of three different particle size distributions (I,III,V) and di-sodium hydrogen phosphates (Na_2HPO_4, analytical reagent, Riedel-de Haën AG, Seelze, Germany) with three different levels of hydrate water (anhydrate, dihydrate and heptahydrate) (IV) were used as model test materials.

4.2 Multichamber microscale fluid bed

A novel multichamber microscale fluid bed device (MMFD) (Ariacon Oy, Turku, Finland) module uses four fluidisation chambers (III-V). The air flow rate and the temperature of the inlet air was individually controllable in each of the chambers. The MMFD module was connected to a process air control unit (Ilmasäätö Oy, Turku, Finland) for controlling the moisture content of the incoming process air (IV, V). Due to the precisely controlled air flow, no filter bags are needed in the fluidisation chambers.

Process control and monitoring was automated, and measured parameters were logged. The automation, instrumentation and process data management of the MMFD was designed using the outlines described in the User Requirements Specification (URS, by Good Automated Manufacturing Practise, GAMP, 1996), Rantanen *et al.* (2000b) and Ruotsalainen *et al.* (2002). The schematic diagram of one fluidisation unit is presented in Fig. 6.

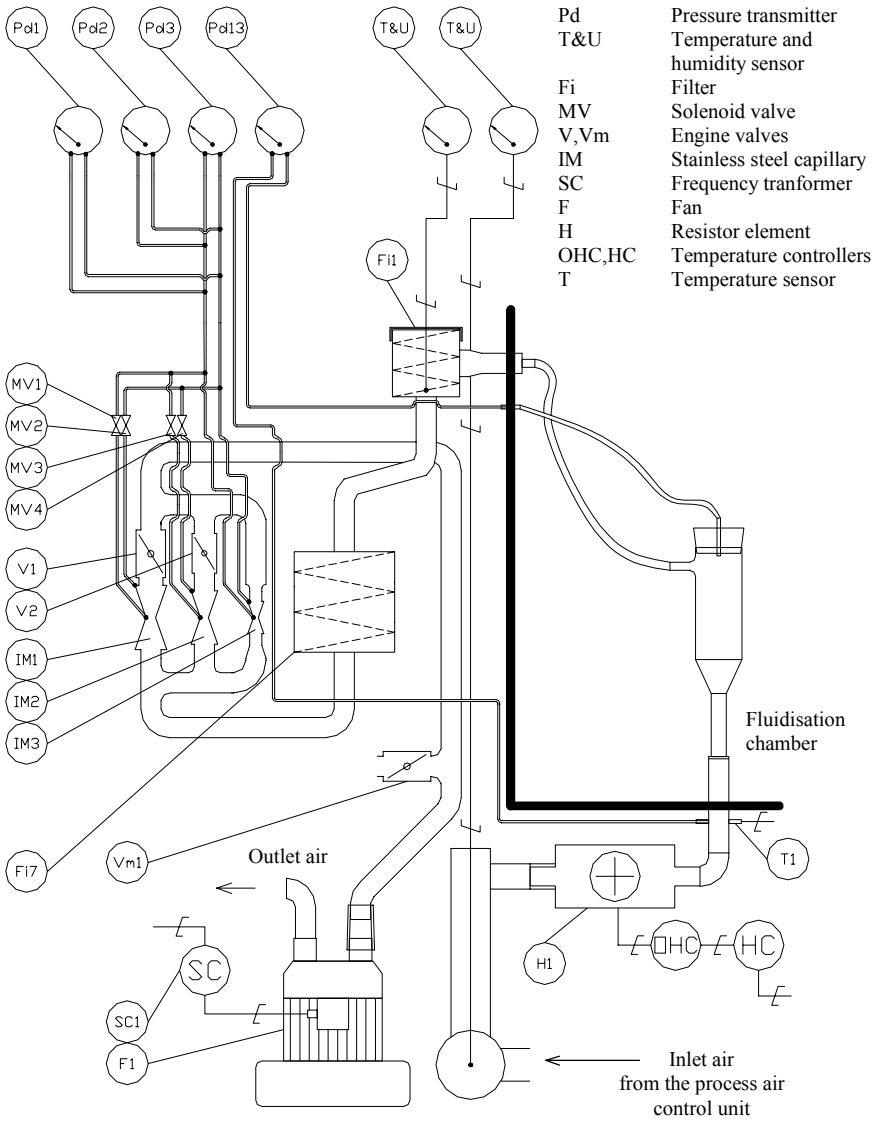

Figure 6. The schematic diagram of one fluidisation unit of a multichamber microscale fluid bed device (MMFD).

The air flow was created with a fan and measured by a high accuracy meter (Ilmasäätö Oy, Turku, Finland) (Fig. 6). The size and the structure of the metering unit

were optimised off-line and calibrated against a valid reference (Gilibrator-2, Sensidyne, Clearwater, Florida, USA). The velocity of the fluidising air was calculated by the measured air flow rate and by the inner diameter of the chamber. The pressure drop over the bed (between the air distributor and the top of the fluidisation chamber) was measured.

Relative humidities and temperatures of the inlet and outlet air were measured using Humicap 233 sensors (Vaisala Oyj, Vantaa, Finland). The sensors were calibrated with a humidity calibrator (HMK15, Vaisala Oyj, Vantaa, Finland). Absolute humidity (g water/m^3 of dry air) and the dew point (°C) of the inlet and outlet air were calculated.

The inlet air of each fluidisation unit was heated to the desired temperature using a resistor type heating element. A temperature controller and a Pt-100 type sensor (Mikor, Turku, Finland) controlled the temperature of the inlet air. The temperature sensors were calibrated using three-point calibration.

4.2.1 *In-line* NIR moisture measurement

In-line moisture measurement (IV) was performed using a multi-channel near infrared (NIR) spectroscopy with a fiber optic probe (Prototype, VTT Electronics, Finland) (Rantanen *et al.*, 1998). Using three wavelengths, the apparent absorbance of water (AWA) was calculated as follows

$$AWA = \frac{-\log(\frac{I_x}{I_{x,ref}}) + \log(\frac{I_y}{I_{y,ref}})}{-\log(\frac{I_z}{I_{z,ref}}) + \log(\frac{I_y}{I_{y,ref}})} \qquad (16)$$

where I is intensity (x refers to the 1998 nm signal, y the 1813 nm signal and z the 2214 nm signal) and ref is intensity using an aluminium column reference at the corresponding wavelength channel (Rantanen *et al.*, 2000b). The reflectance at 1998 nm was used as a water indicator. The reflectance at 1813 nm was used for baseline correction and the reflectance at 2214 nm for normalisation. The measurements were performed through the fluidisation chamber made from glass (Fig. 7).

Figure 7. Experimental set-up (IV, V).

4.2.2 *Non-invasive* electrostatic measurement

A ring probe (III) was utilised to measure the net charge distribution along the fluidisation chamber *non-invasively* (Fig. 8). The induction ring was located vertically in the middle of the probe and electrically isolated from the case with polytetrafluoroethylene (PTFE). The brass case was grounded and the induction ring was connected to an electrometer (Keithley 6514, Keithley Instruments Inc., USA). The ring probe was used to sense both the charge of the powder and the charge of the insulating pipe. However, the pipe was closer to the induction ring than the powder and therefore the measured signals were more sensitive to the charging of the pipe surface. The detailed model of the measurement system was composed using an advanced field solving

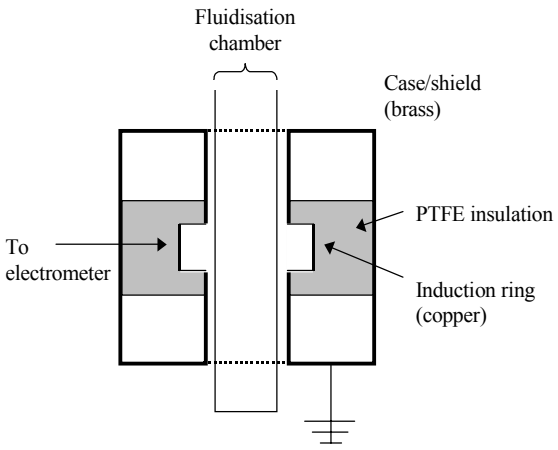

Figure 8. Schematic diagram of the ring probe.

software based upon the finite element method (OPERA-2D, Vector Fields Ltd., Oxford, UK). Different parameters, such as the height of the bed, the initial charge of the powder and the relative permittivities of the powder and the column, were adjusted.

4.3 Process conditions

The batch sizes of the studied materials (III-V) were from 2 to 15 grams. The electrostatic measurements were performed at ambient conditions (III). The fluid bed drying (IV) was performed in dry air (< 0.5 g water/m^3 of dry air) and in increased moisture content (10.3 g/m^3 ± 0.2 g/m^3) of the inlet air. The effect of the temperature of the inlet air (from 30 °C to 90 °C) was also evaluated. The fluidisation behaviour (V) was determined at two different moisture contents of the inlet air, dry air and air containing water 9.5 g/m^3 (± 0.2 g/m^3). To minimise the effect of packing, the fluidisation behaviour (V) of the materials was determined from the decreasing velocity of the process air (Kunii and Levenspiel, 1991). Air flow rates were selected so that the fluidisation occurred mainly at the lower part of the chamber (IV, V).

4.4 Characterisation of materials

Moisture contents (I, II, IV) were determined using an infrared dryer (Sartorius Thermocontrol YTC01L, Sartorius GmbH, Göttingen, Germany). The infrared dryer heated the samples until the loss of weight was less than 0.1 % in 50 s. The measurements were made in triplicate and the results were the average of the determinations (± standard deviation, SD).

The true density (I, III, V) of materials was measured using a pycnometer (Micromeritics, Model 1305, Norcross, GA, USA). The density results were the averages of three different determinations. Bulk volume (I) was determined by pouring 50 g of material into a 250 ml glass measuring cylinder held at an angle of 45° to the horizontal while pouring. After pouring, the measuring cylinder was brought to a vertical position and the bulk volume was determined. Tapped volumes were measured using a standardised tapped density tester (Erweka SVM1, Erweka GmbH, Heusenstamm, Germany) in which the glass measuring cylinder was tapped 500 times (I).

Particle size and size distributions (I, III, V) were determined by a laser light diffractometer (Malvern 2600C droplet and particle sizer, Malvern Instruments Ltd., Malvern, UK). The method of determination was particles in air. On the basis of the mean particle sizes and the true densities, the materials (V) were classified into different groups, according to the Geldart (1973) classification. The computational u_{mf} were calculated using Eq. 7, with the experimental constants ($\frac{K_1}{2K_2}$ and $\frac{1}{K_2}$) determined by Wen and Yu (1966) and Chitester *et al.* (1984). The utilised experimental constants were selected from a wide range, so that the computational u_{mf} were calculated as comprehensively as possible.

4.5 FT-NIR spectroscopy

In the first phase (I), the diffuse reflectance NIR spectra were measured with a Fourier Transform (FT)-NIR spectrometer (Bühler NIRVIS, Uzwil, Switzerland) with fiber-optic probe. The diffuse reflectance spectra for solids and the transflectance spectra for liquids were measured over the range of 4008-9996 cm^{-1} with a resolution of 12 cm^{-1}. Each individual spectrum was an average of four scans and all measurements were performed five times. The spectral treatment (absorbances and second derivatives) was performed with NIRCAL v. 2.0 (Bühler, Uzwil, Switzerland). In the second phase (II, IV), the NIR spectra were measured with a FT-NIR spectrometer (Bomem MB-160 DX, Hartman & Braun, Quebec, Canada). The spectra were measured in triplicate through the bottom of a glass vial between 4000-10000 cm^{-1} with a resolution of 16 cm^{-1}. The samples were scanned 32 times and each spectrum was reported as the average of these scans. Standard reflection was measured using Teflon (99% reflective Spectralon, Labsphere, North Sutton, USA) background. Spectral treatment was performed using Bomem Grams/32 software (v. 4.04, Galactic Industries corp., Salem, NH, USA).

4.6 X-ray diffraction

X-ray diffraction patterns of the theophylline granules (II) were measured using a wide-angle X-ray scattering (WAXS) theta-theta diffractometer (Seifert XRD 3000, Rich. Seifert & Co., Germany). The WAXS experiments of the samples were performed in a

symmetrical reflection mode with CuK_α radiation (1.54 Å) monocromatised with a graphite monochromator in the scattered beam. The scattered intensities were measured with a NaI(Tl) scintillation counter. The angular range was from 2^o to 20^o (at θ) with steps of 0.03^o, and the measuring time was 15 s/step at all measurements. The amounts of anhydrous theophylline and theophylline monohydrate in the granules were estimated by fitting a linear combination of the diffraction patterns of the anhydrous theophylline and theophylline monohydrate to the diffraction patterns of the granules (Matlab v. 5.3, The MathWorks, Inc., Natick, MA, USA).

X-ray diffraction studies of the phosphate samples (IV) were made using an X-ray diffraction (XRD) theta-theta diffractometer (Bruker axs D8, Karlsruhe, Germany) with Göbel Mirror bent gradient multilayer optics. The scattered intensities were measured with a scintillation counter. All the experiments were performed in symmetrical reflection mode with CuK_α radiation (1.54 Å), and the angular range was from 8° to 42° (2θ) with increments of 0.05°. The measuring time was 1 s/increment.

4.7 Differential scanning calorimetry

Differential scanning calorimetric (DSC) measurements (II) were performed on a Mettler DSC analyser (model 821^e, Mettler Toledo Ag, Switzerland) using STAR software (STAR 5.1, Sun Soft Inc., USA). The temperature axis of the equipment was calibrated with zinc and indium, and the thermobalance with calcium carbonate. The runs were performed under nitrogen gas flow (50 ml/minute) in open aluminium pans, and the weights of the samples were 3-5 mg. The heating rate was 10 °C/min over the temperature range of 25-300 °C.

5. RESULTS AND DISCUSSION

5.1 Studying water-solid interactions using NIR spectroscopy

Understanding the nature of the process environment is necessary when the NIR set-up is applied for pharmaceutical *in-line* measurements. Watano *et al.* (1996a) have studied the effect of aqueous granulation liquid flow rate and the temperature of process air for fluid bed granulation using NIR spectroscopy. The suitable amount of water addition for wet granulation has also been evaluated using NIR measurements (Miwa *et al.*, 2000). However, it has been noticed that water molecules can associate with solids in different ways (Zografi, 1988). Adsorbed water molecules interact only with the surface of a solid. Absorbed water molecules penetrate into the bulk solid structure, and they may cause changes in the crystal structure. The fact that water molecules may influence the behaviour of drugs (Haleblian and McCrone, 1969; Grant, 1999) increases the demand to study the state of water during pharmaceutical processes in more detail.

The characterisation of the state of an active pharmaceutical ingredient (API) or bulk drug is important (Byrn *et al.*, 1995; Yu *et al.*, 1998; Byrn *et al.*, 1999). Phase transitions such as the transformation of a polymorph, the formation of a hydrate or the desolvation of a solvate may occur during various processes, *e.g.*, during tableting, wet granulation or drying (Morris *et al.*, 2001). Traditionally, the phase transitions of APIs have been studied using infrared (IR) spectroscopy, thermal methods, optical and electron microscopes, nuclear magnetic resonance spectroscopy, and X-ray diffraction (Brittain *et al*, 1991; Roston *et al.*, 1993; Nguyen *et al.*, 1994; Morris *et al.*, 1994; Madan and Kakkar, 1994; Yu *et al.*, 1998). These methods are reliable but relatively slow, and limited to *off-line* and *at-line* applications. To understand the basis of the polymorphism at the molecular level and to predict and prepare the most stable form of drug for development, detailed knowledge from the processing-induced transformations (PITs) are required.

The different energetic states of water molecules have been studied using the second derivative of the NIR absorbance spectra (Iwamoto *et al.*, 1987; Maeda *et al.*, 1995; Luukkonen *et al.*, 2000; Jørgensen *et al.*, 2002). NIR spectroscopy has also been applied for studying the polymorphism and pseudopolymorphism of different pharmaceutical materials (Aldridge *et al.*, 1996; Buckton *et al.*, 1998; Jørgensen *et al.*,

2002). Luner *et al.* (2000) and Seyer *et al.* (2000) have determined the accuracy of the NIR as a tool for quantifying the different crystalline forms of solids in binary mixtures. However, moving the NIR measurement to the process environment may increase the prediction error of the calibration models and then, the issues related to sample representativeness and the process interface should be considered.

Monitoring the water-solid (drug) interactions *in-line* allows a potent tool for improving the processes and the quality of final products (Morris *et al.*, 1998). In this chapter, the effect of particle size and binder (granulation liquid) on the *in-line* NIR moisture measurement was evaluated (I). Further, NIR spectroscopy was utilised for the characterisation and the monitoring of the phase transformations of a model drug molecule (theophylline) during two different pharmaceutical unit operations (II, IV).

5.1.1 Evaluation of spectral factors

NIR moisture measurements can be performed with constructions applying only few measured wavelengths (Watano, 1995; Watano *et al.*, 1996a; Watano *et al.*, 1996b; Rantanen *et al.*, 1998; Miva *et al.*, 2000; Rantanen *et al.*, 2000a). In such cases, the calibration can be done by combining the measured wavelengths into a baseline corrected absorbance value, which is further calibrated against a valid reference technique. In addition to the detection of the water signal, the baseline correction signal is needed in order to correct the offset in the spectra baseline. However, the utilisation of NIR spectroscopy for *in-line* applications and process optimisation requires understanding all factors affecting the radiation.

Due to the minimal absorbance in the NIR region, the inorganic glass beads proved an advantageous compound for the evaluation of spectral factors (I, Fig. 1). The effect of particle size differences was noticed on the general baseline of the spectra. When the light was penetrated deeper into the sample due to the increasing particle size (Williams and Norris, 1987), more absorption occurred and an apparent increase in absorbance was observed.

The glass beads also reveal the spectral phenomena during wet granulation (I, Fig. 3a). Water bands (at around 1450 nm and 1940 nm) were a major spectral feature of the inorganic glass beads. Water within the inorganic material was adsorbed and the

continuous water film around the glass beads affected the back reflected light. The change in the physical properties of the sample resulted in the upward shift of the spectra baseline. The increase of the baseline was due to the change in the refractive index discontinuities. The change in refractive properties affected the effective path length and resulted in an apparent increase in absorbance in the whole spectra. The same phenomena were observed with MCC (I, Fig. 3b) and with theophylline (Fig. 9), but not in the same extent. In the case of pharmaceutical solids, water molecules were absorbed within cellulose fibres (Froix and Nelson, 1975; Zografi *et al.*, 1984; Fielden *et al.*, 1988; Blair *et al.*, 1990) and within tunnels (Sun *et al.*, 2002) formed by surrounding theophylline molecules (the formation of theophylline monohydrate).

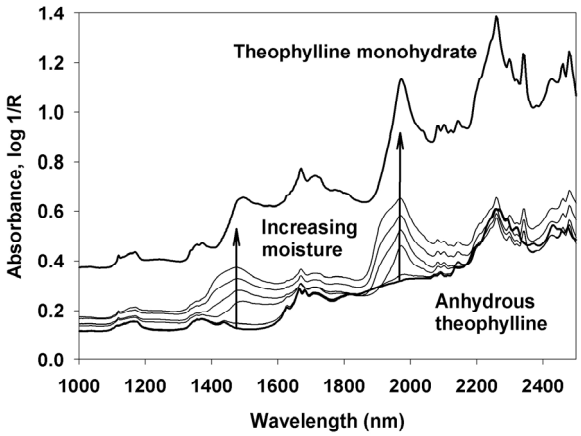

Figure 9. NIR spectra of anhydrous theophylline, theophylline monohydrate (needle-like), and wet theophylline granules.

The comparison of second derivative difference spectra enables the identification of binder effects on the FT-NIR spectra of granulated materials (I, Figs. 4 and 5). With the glass beads, the spectral effects of PVP were recognised at around 1700 nm (first overtones of CH stretches) and 2200 nm (combinations of CH, OH and CO stretches and deformations) (I, Fig. 4b) (Williams and Norris, 1987; Osborne *et al.*, 1993). When pharmaceutical material with absorbing nature (MCC) was studied (I, Fig. 5), the effects were not as visible as with non-absorbing glass beads.

Studying the physicochemical background affecting the NIR spectra enables a reliable utilisation of the *in-line* measurements. The particle size and the binder effects should be considered when the spectral response of the NIR moisture measurement is calibrated. In the first phase, understanding the nature of water-solid interactions could be easier when the measurements are performed *off-line*. The use of well-studied *in-line* methods may facilitate achieving the essential knowledge from the PITs of the pharmaceutical solids.

5.1.2 Determination of hydrate formation during wet granulation

Theophylline has been extensively studied as a model drug molecule. It is well known that anhydrous theophylline transforms rapidly into theophylline monohydrate when in contact with water molecules. During the pelletisation process and storing of tablets under elevated humidity conditions, the phase transformation of anhydrous theophylline into theophylline monohydrate has been established (Herman *et al.*, 1988; Ando *et al.*, 1992; Otsuka *et al.*, 1992). The thermal dehydration product of theophylline monohydrate (metastable form of anhydrous theophylline) in tablets has also been found (Phadnis and Suryanarayanan, 1997). Among these different forms and their mixtures, different release rates and solubilities have been reported (Shefter and Higuchi, 1963; Bogardus, 1983; Herman *et al.*, 1988; Zhu *et al.*, 1996; Phadnis and Suryanarayanan, 1997).

During the wet granulation of anhydrous theophylline, the transformation of theophylline monohydrate was observed in the second derivative of absorbance at around 1475 nm and 1970 nm (Fig. 10). When the moisture content of the theophylline granules was low, the absorption increased only at these wavelengths. Also, some changes in the baseline of the spectra occurred due to the increasing particle size of granules (Norris and Williams, 1983; Ciurczak *et al.*, 1986; Osborne *et al.*, 1993; Frake *et al.*, 1997; Gaines and Windham 1998).

When the moisture content of the wet theophylline granules was increased up to 1.3 moles of water per mole of anhydrous theophylline, new absorption maxima were observed at

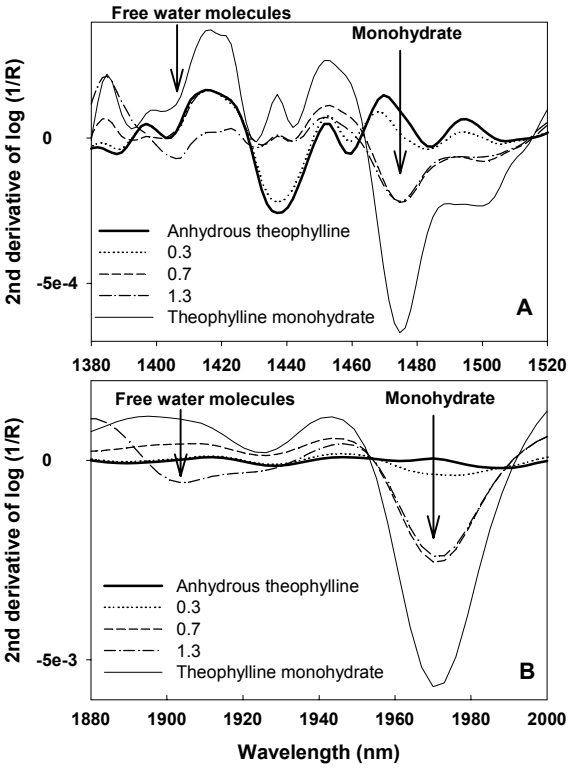

Figure 10. Transformation of anhydrous theophylline into theophylline monohydrate at around 1475 nm (A) and 1970 nm (B). Free water molecules are detected at around 1410 nm (A) and at around 1905 nm (B). Numbers indicate the amount of water (mole(s) of water per mole of anhydrous theophylline).

around 1410 nm and 1905 nm (Fig. 10). The intensity of the absorption maxima of theophylline monohydrate remained constant. These new absorption maxima were due to OH vibrations of free water molecules. After this, increasing the moisture content of the theophylline granules, the spectral baseline also increased due to the changes in refractive index discontinuities and increasing particle sizes (Fig. 9).

In theory, all anhydrous theophylline should be transformed to theophylline monohydrate when the moisture content of the granules was increased up to one mole of water per one mole of anhydrous theophylline. However, it is concluded that not all anhydrous theophylline was transformed to theophylline monohydrate, and there were some dry regions inside the granules. DSC and X-ray diffraction confirmed all the findings and conclusions made by FT-NIR spectroscopy (II, Figs. 4 and 5).

The demand to investigate the PITs has generated a special need for new measurement technologies. Using FT-NIR spectroscopy the hydration of anhydrous theophylline into theophylline monohydrate was observed at around 1475 nm and 1970 nm. Free water molecules were observed at around 1410 nm and 1905 nm. Recently, Jørgensen *et al.* (2002) have studied the hydrate formation of caffeine during wet granulation and have established the phenomena to the structurally related drug compound. It is concluded that the fast and flexible NIR spectroscopy is a promising tool for studying the water-drug interactions during processing.

5.1.3 *In-line* monitoring of fluid bed drying in microscale

In the previous chapters the spectral factors affecting *in-line* NIR moisture measurement have been evaluated and the determination of the PIT of theophylline by FT-NIR spectroscopy has been described. The purpose of this chapter is to connect this knowledge to the monitoring of the fluid bed drying behaviour of pharmaceutical (theophylline) granules. The experiments were performed in the developed microscale fluid bed and the results were evaluated on the basis of *in-line* NIR moisture measurement.

Before the fluid bed drying, the wet theophylline granules included free water and monohydrate water molecules (IV, Table 3. and Fig. 6). When the granules were dried in dry air (< 0.5 g/m^3) and in the low temperature of the inlet air (35 °C), the

equilibrium moisture content and the FT-NIR spectra of the granules approached that of anhydrous theophylline. When the moisture content of the process air was increased to 10.3 g/m^3, only the free water molecules of the wet theophylline granules were evaporated. The moisture content of the granules stayed constant for several hours and approached the computational moisture content of theophylline monohydrate, understandably 9.1% (IV, Table 3). The FT-NIR spectra confirmed that these granules were consisted mainly of theophylline monohydrate (IV, Fig. 6).

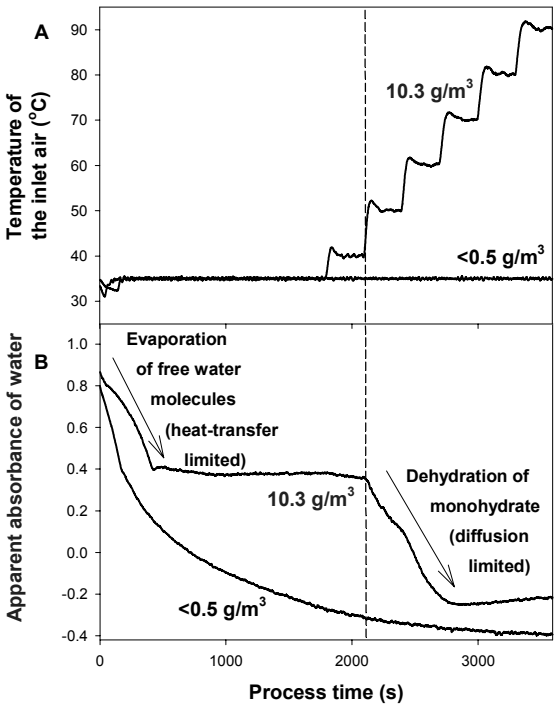

Figure 11. Wet theophylline granules dried in two different moisture contents, <0.5 g/m^3 (dry air) with constant temperature (35 °C) and 10.3 g/m^3 with increasing temperature (from 35 °C to 90 °C). A) Temperature of the inlet air B) Apparent absorbance of water (AWA) value during processing.

The behaviour of the wet theophylline granules during the fluid bed drying was studied by increasing the temperature of the inlet air step by step (Fig. 11). The evaporation of free water molecules was detected when the apparent absorbance of water (AWA), measured by *in-line* NIR spectroscopy, decreased to a constant level at around 0.4. This phase of drying was a heat-transfer limited (Davidson *et al.*, 1985; Kunii and Levenspiel, 1991; Yang, 1999). The step was distinct when the moisture content of the process air was 10.3 g/m^3 and the temperature of the inlet air was low (35 °C). In these process conditions, the dehydration of theophylline monohydrate (diffusion limited phase) began by increasing the temperature of the inlet air.

The dehydration of theophylline monohydrate has been established to be a two-step process (Suzuki *et al.*, 1989; Duddu *et al.*, 1995; Suihko *et al.*, 1997). The first step is the breaking of the hydrogen bonds between the theophylline and the water molecules, and the second step is the evaporation of the loosened water. In practice, these steps of dehydration are overlapping. When the wet theophylline granules were dried in the dry

air, a weak point of inflection of AWA at around 0.4 was observed. The different steps of drying, the evaporation of free water molecules and the dehydration of theophylline monohydrate, were overlapping. It is suggested that the stepwise (overlapping) drying behaviour may be partly responsible for the non-linearity of the spectral response reported during fluid bed granulation process of theophylline (Rantanen *et al.*, 2001a).

Rantanen *et al.* (2000b) have studied the fluid bed granulation process of theophylline in a pilot-scale with the equal *in-line* NIR moisture measurement set-up. The value of AWA and the moisture contents of the theophylline granules were in accordance with these results, which suggested that the basic phenomena in microscale are closely related to the larger scale. However, it was observed that the moisture content of the inlet air had an effect on the value of AWA. The difference was remarkable at the low level of the moisture content of the theophylline granules. One explanation is the influence of the moisture content of the inlet air on the fluidisation and packaging behaviour (adhesion and cohesion) of the anhydrous theophylline granules. Because the low drying temperature and the low humidity of the process air increases the transformation of metastable forms (Morris *et al.*, 2001), the effect of polymorphism on the fluid bed process behaviour should be studied. The multivariate process monitoring solutions, *e.g.* principal component analysis (Rantanen *et al.*, 2000b) and self-organising maps (Rantanen *et al.*, 2001b) could be used to deduce the properties of the final product from the correlations of the process parameters or conditions.

The results established that *in-line* NIR spectroscopy is a valuable tool for studying the PITs of API. During fluid bed drying, two different drying phases of the wet theophylline granules were observed and verified (IV, Table 3, Fig. 6 and 7). The first step was the rapid evaporation of free water molecules and the second step the slow dehydration of monohydrate water molecules from the tunnels formed by surrounding theophylline molecules (Sun *et al.*, 2002). The moisture content of the inlet air had a significant effect on the drying behaviour of the wet theophylline granules. It is concluded that when measuring the moisture content *in-line*, three carefully selected wavelengths from the NIR region are sufficient. Fundamental advantages could be achieved by the speed of analysis and instrument expenses. It is suggested that controllable and monitored fluid bed conditions on a microscale might give useful information, which can be used for scale-up and process optimisation studies in preformulation stage.

5.2 Studies using a multichamber microscale fluid bed

In early drug development stages, new molecules are expensive and their availability is often limited to few grams. Despite the fact, the characterisation of the formulations should be as extensive as possible (Brittain *et al.*, 1991). The trend to emphasise the preformulation stage requires new technologies that enable smaller amounts of samples to be studied, analysed and processed (Alkan *et al.*, 1988; Hancock *et al.*, 2000; Rowe, 2000; Bock and Kraas, 2001, Mackin *et al.*, 2002). The purpose of this chapter was to develop an automated and instrumented multichamber microscale fluid bed set-up for the preformulation studies of the pharmaceutical solids. The experiments were performed with grams (from two to seven grams) of pharmaceutical material in monitored and controlled process air conditions.

5.2.1 Electrostatic measurements

The electrostatic charging of materials during processing presents a fundamental problem to the pharmaceutical industry (Hearn, 1998). Previously, the charging behaviour of fluid beds have been studied by taking samples from the bed (Ali *et al.*, 1999), by measuring the electric field from the side of the chamber (Watano *et al.*, 1998) or by an electrode inside the bed (Ciborowski and Wlodarski, 1962; Kiselnikov *et al.*, 1967; Fujino *et al.*, 1985). However, these methods have some disadvantages, *e.g.*, taking the sample inevitably changes the charge on the sample, field meters can not be used inside the powder volume, particles adhere to the electrodes, and contact charging takes place between the particles and the electrodes. Also, most of these methods interfere in the fluidisation process and therefore the techniques are difficult to utilise in small-scale. This chapter describes and evaluates the applicability of *non-invasive* electrostatic measurement technique, the ring probe (Fig. 7), for the microscale fluid bed and for the formulation studies of pharmaceutical solids.

The signal of the ring probe was assessed with a charged water droplet and with a charged acrylic chamber. The results indicated that the closer a measured charge located, the better the resolution of the ring probe was (III, Fig. 3). The probe sensed the electric field of the bed from a relatively wide region, and a relatively narrow region from the surface of the chamber.

The simulations established the detailed model of the electrostatic measurement (III, Fig. 4). At the low level, the ring probe sensed the negative charge on the surface of chamber. Moving the probe above the bed level, the field lines arising from the positive particles coupled with the induction ring. When the negative charge was distributed on a broader area than the bed of solid particles, curves changed direction. This was due to the reduced negative charge at the bed level and increased negative charge above the bed level. When the height of the charged area of the chamber was equal with the height of the bed, the opposite charges on the wall and on the particles almost counterbalanced each other (III, Fig. 5). Thus, measured signals could be considered as the sum of two charged regions.

Simulated curves were quite similar with the experimental results (III, Fig. 10). The glass beads were charged negatively (Fujino *et al.*, 1985) and so, the acrylic chamber received a positive charge when in contact with the glass beads (III, Fig. 8). When the velocity of the inlet air was increased, the glass beads fluidised upwards and hit the wall of the chamber leaving a positive charge. At first, the signal was negative but when the fluidisation proceeded and the velocity increased, the signal turned clearly positive (above the level of the bed). It was concluded that the specific charge of the glass beads increased with an increasing velocity, as has been shown previously (Ciborowski and Wlodarski 1962; Kiselnikov *et al.*, 1967).

The charging profile of the chamber was used to study the charge of the glass beads. The negative specific charge was linearly related to the area between the fill curve and the charging curve after the fluidisation (III, Fig. 9.). However, simulations showed that the integrated area depends not only on the charge, but also on the way the charge was distributed. To determine the exact amount of initial and transferred charge, a more complicated method should be used.

Microcrystalline cellulose carried a positive initial charge before fluidisation started in an acrylic chamber (III, Fig. 6). During fluidisation, curves shift to a negative direction. This implies that the acrylic column received a negative charge and therefore the powder received a positive charge. When the microcrystalline cellulose powder was fluidised, particles hit the column wall above the bed level leaving a negative charge on the surface of the chamber. Similar results (the curves were oriented the other way around) were obtained with the glass beads (III, Figs. 8 and 9). After filling there was a

negative peak, which began to move towards positive values and at the same time a positive peak grew above the bed level.

Lactose monohydrate was charged negatively in a glass chamber. The charge signals begin to move to a positive direction within the bed due to the positive charging of the glass chamber when in contact with the lactose particles (III, Fig. 11). However, above the bed level the curves moved to the negative direction. This behaviour was due to the strong adhesion of negatively charged particles on the column surface. Unlike glass beads or microcrystalline cellulose in an acrylic column, lactose particles did not hit the wall of the chamber and then return back to the bed. When they contacted the wall, they adhered to it and their negative charge was measured. It was concluded that the charging curves of successive experiments interacted with each other near the top of the bed of solid particles. Above the bed level signals originated either from the impacts between the particles and the wall of the chamber or from the adhesion of charged particles on the surface of the chamber. It was noticed that if the charging curves of successive experiments influenced each other, the signal was due to adhesion.

The ring probe was also used to study the charge generation at a chosen location as a function of time (III, Fig. 7). The result indicated that with the glass beads, the main charging takes place very quickly (under 60 seconds) and only slight charging behaviour (continuous process) was observed after two minutes. The developed method for continuous electrostatic charge measurements could be a helpful tool for revealing a better understanding of the complex charging behaviour of pharmaceutical solids. It is suggested that the *non-invasive* arrangement might give advantageous results for the studying of the effect of formulation or process conditions on the charging behaviour during processing.

5.2.2 Dehydration studies

Fluidisation has been utilised extensively for drying because of its large capacity, reasonable low capital cost and high heat and mass transfer (Kunii and Levenspiel, 1991). However, the analysis of fluid bed drying is complicated, due to the fact that different drying regimes may be observed successively. Controlling and monitoring the drying conditions of pharmaceutical materials is important, since the conditions have significant effects on the properties of the final products (Morris *et al.*, 2001). To

optimise the fluid bed drying processes and the properties of the final products, exact information from all process phases and conditions during this multivariable process is required.

The dehydration of Na_2HPO_4 with three different levels of hydrate water was studied using the multichamber microscale fluid bed. The moisture difference between the inlet and outlet air demonstrated the dehydration behaviour of Na_2HPO_4 dihydrate (IV, Fig. 2A). By computing the mass balance from the moisture difference, it was possible to follow the stage of dehydration during processing (IV, Fig. 2B). As expected, increasing the temperature of the inlet air increased the dehydration rate. In addition, using a trivial assumption of first order kinetics, the activation energy of dehydration was obtained (42 kJ/mol). It is suggested that with such an arrangement, fundamental advantages could be obtained for studying the dehydration kinetic of drugs during real pharmaceutical unit operation.

Drying Na_2HPO_4 heptahydrate in various temperatures, two equilibrium moisture contents of the final product were obtained (IV, Table 2). When the temperature of the inlet air was low (≤ 40 °C), the equilibrium moisture content of Na_2HPO_4 heptahydrate was reached at Na_2HPO_4 dihydrate. Increasing the temperature of the inlet air to 50 °C, the equilibrium moisture content was equal to that of anhydrous Na_2HPO_4. Increasing the temperature of the inlet air step by step, the dehydration of Na_2HPO_4 heptahydrate was monitored by the peak value in moisture difference during processing (IV, Fig. 5). The first peak value of the moisture difference was due to the dehydration of Na_2HPO_4 heptahydrate to Na_2HPO_4 dihydrate, and the second one was due to the dehydration of Na_2HPO_4 dihydrate to anhydrous Na_2HPO_4. Accordingly, two distinct decreases in pressure difference over the bed were due to the same phase transition. However, the decreases of the pressure difference were not directly proportional to the decreases of the moisture contents (IV, Table 2 and Fig. 5). This was probably due to significant changes in interparticle forces (*e.g.*, liquid bridges and electrostatic charging) during processing. The XRD patterns and the FT-NIR spectra established the dehydration behaviours (IV, Figs. 3 and 4).

Otsuka and Kaneniwa (1990) suggested that the hygroscopicity and the chemical stability of cephalothin sodium in the solid state are closely related to its crystallinity. Also, the particle size and the lattice integrity have an influence on phase transitions and dehydration kinetics of trehalose dihydrate (Taylor and York, 1998a; Taylor and York,

1998b). It is suggested that the explanation for the lower dehydration temperatures of Na_2HPO_4 heptahydrate with 19.3% of water (50 °C) in comparison with Na_2HPO_4 dihydrate (60 °C) could be different crystal sizes and the crystallinity of the phosphates (IV, Table 2). The suggestion emphasised the fact that when processing materials that are sensitive to phase transitions, the determination of the true process behaviour is extremely important.

The developed multichamber microscale fluid bed proved to be an advantageous device for studying the dehydration behaviour during processing. As it was earlier established with wet theophylline granules, the microscale set-up offers fundamental advantages for studying the fluid bed drying behaviour of pharmaceutical materials in variable conditions using only grams of material for analysis. Measuring the pressure difference over the bed was proved to be a useful additional method for monitoring the fluid bed drying.

5.2.3 Characterisation of fluidisation behaviour

The different interactions and interparticle forces of the pharmaceutical solids can cause serious problems during fluid bed processes. Although various theories for factors affecting the fluidisation are available, the basic understanding of the underlying mechanisms is yet to be discovered. Until the gap between theory and practice is bridged, the detailed process behaviour of pharmaceutical materials must be determined experimentally.

The applicability of the multichamber microscale fluid bed for the characterisation of the fluidisation behaviour was studied on the basis of two common computational methods (Davidson *et al.*, 1985; Kunii and Levenspiel, 1991; Yang, 1999), the minimum fluidisation velocity (u_{mf}) and the Geldart classification. With the model particles (glass beads), different characteristic phases (*e.g.*, plugging, bubbling, slugging and turbulent fluidisation) of the fluidisation were observed and identified. The experimental u_{mf} of larger glass beads (2 and 3) were predicted well by the computational u_{mf} (V, Table 3) and the fluidisation behaviours of these glass beads were classified on the basis of the Geldart classification (V, Figs. 2 and 3BC). However, the behaviour of finest glass beads (1) was not accurately predicted or classified by the computations (V, Table 4, Figs. 2 and 3A). Zhou and Li (1999) have suggested that when the particle size of

cohesive particles is decreased, the interparticle forces increase making the fluidisation behaviour worse. One explanation for the unsuitability of the computational methods is charging behaviour, due to the fact that the studied materials are electric insulators.

The fluidisation behaviour can be monitored and followed on the basis of the pressure difference over the bed as a function of the fluidisation air velocity (V, Fig. 3). The same technique can also be used for monitoring the dehydration behaviour during fluidisation (IV, Fig. 5). With such an arrangement, fundamental advantages could be achieved when visibility inside the fluidisation chamber is limited and other process monitoring techniques are inadequate. However, the utilisation of this technique requires precisely controlled and monitored process conditions.

It has been established that the moisture content of the process air has various effects on the powders' behaviour during processing (Dawoodbhai and Rhodes, 1989). Geldart *et al.* (1984) state that most group A particles can be made to behave like cohesive group C particles by fluidising them with air of the relative humidity of 60 to 90%. This is due to the effect of capillary condensation (liquid bridges) on the fluidisation behaviour. In the dry air (< 0.5 g/m^3) of fluid bed, all the glass beads adhered to the wall of the chamber as a thin layer, and the finest glass beads (1) cannot properly be fluidised (V, Fig. 3A). The adhesion was also observed with the largest glass beads (3) by the decreasing pressure difference over the bed at the highest fluidisation velocities (V, Fig. 3C). When the amount of charge carriers (water molecules) in the process air was increased (9.5 g/m^3), the effect of cohesion and adhesion was diminished (V, Figs. 3 and 4). This was due to decreasing electrostatic forces. With the larger glass beads (2 and 3), the decreasing resistance of fluidisation was also observed by the decreasing experimental u_{mf} (V, Table 3). The observations were in agreement with studies made using a cyclone apparatus, where the charge of α-lactose monohydrate was decreased when the humidity in the apparatus was increased from 2 % to 100 % relative humidity (Eilbeck *et al.*, 2000).

Controlling and monitoring the process air conditions, *e.g.*, during coating and granulation, is important (Yang, 1999). Although the van der Waals forces have been established to be dominant during powder handling and fluidisation (Bailey, 1984; Visser, 1989), the electrostatic forces has been demonstrated to be a significant factor when electric insulators are in contact with each other. It is suggested that when the

fluidisation air is precisely controlled and monitored, fundamental information about the charging behaviour of fine solid particles can be obtained.

Microcrystalline cellulose (MCC) is widely used as an excipient in the pharmaceutical industry. By co-processing MCC with a colloidal silicon dioxide, *e.g.*, the compaction properties of standard MCC have been improved (Sherwood and Becker, 1998). The silicon dioxide improves the flowability and increases the specific surface area of SMCC particles compared to MCC. Due to the adhesion and cohesion of MCC powders (Fig. 12), the computation of u_{mf} and the prediction of the fluidisation behaviour (the Geldart classification) of MCC on the basis of the mean particle sizes and the density differences were difficult (V, Table 4, Figs. 6). With SMCC powders, adhesion and cohesion was reduced and the fluidisation behaviours were predicted well by the Geldart classification. Also, the experimental u_{mf} of the SMCC were closer to the computational u_{mf} than the MCC powders. It is concluded that the SMCC have better fluidisation properties than the standard MCC powders, even though the silicification process has been established to produce a material, which is chemically and physically very similar to standard MCC powder (Tobyn *et al.*, 1998).

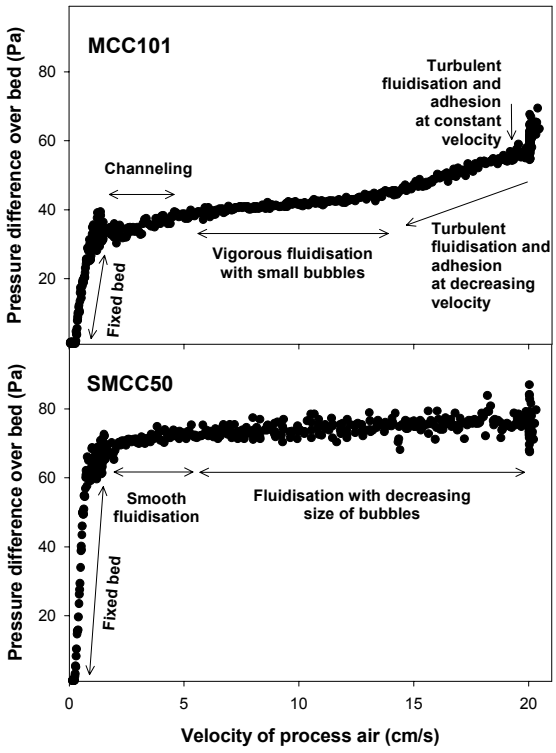

Figure 12. Fluidisation behaviour of microcrystalline cellulose (MCC101) and silicified microcrystalline cellulose (SMCC50) in dry process air (moisture content < 0.5 g/m^3).

The location of the silicon dioxide is primarily on the surface of MCC particles (Edge *et al.*, 1999). The better compaction properties of SMCC have been explained by interfacial interactions rather than modification of the bulk properties of MCC powders (Edge *et al.*, 2000). However, the detailed mechanism behind the better functionality of SMCC is still unknown. It is suggested that the improved fluidisation behaviour of SMCC was due to the ability of the silicon dioxide to keep some water molecules in the

system (Fig. 12). This leads to increasing amounts of free charge carriers and weaker electrostatic forces on the surface of SMCC particles.

Powders having similar physical properties might have different process behaviour (Fig. 12). Due to the inadequacy of computational methods developed in other industries, the determination of the experimental process behaviour of pharmaceutical powders is extremely important. As was pointed out with the finest glass beads (1), the most reasonable explanation for the unsuitability of the computational approaches was the interparticle forces that resist fluidisation. The fact that the estimations do not take into account particle size distributions, shape distributions or the process conditions (*e.g.*, moisture content) may also be a potential source of error. More knowledge of the interactions and the interparticle forces during the fluid bed processes is needed in order to utilise computational methods for pharmaceutics.

Due to the fact that during fluidisation, solids are exposed to high mechanical stress and the interparticle forces are emphasised, the fluid bed behaviour could be an interesting approach to characterise the process behaviour of pharmaceutical powders. The difference between the experimental and the computational u_{mf} could be a useful parameter. The greater the difference is, the more interparticle forces would appear that would resist the fluidisation. The fact that adhesion and cohesion can cause inadequate flowability (Staniforth, 2000) suggests that the fluidisation behaviour could universally predict pharmaceutical process behaviour. The pressure difference over the bed as a function of fluidisation velocity is established to be a potent approach to characterise the fluid bed process behaviour of pharmaceutical solids even with only grams of materials for analysis.

6. CONCLUSIONS

Understanding the physicochemical background of the NIR spectra enables a reliable utilisation of the *in-line* NIR moisture measurements. The intensively pre-examined *in-line* NIR method facilitates achieving the detailed knowledge from the processing-induced transformations (PITs) of an active pharmaceutical ingredient (API).

The *non-invasive* electrostatic measurement technique allowed to scan the charge across the chamber or to monitor the generation of charge at the chosen location. The technique could be a helpful tool for the understanding of the complex charging behaviour of pharmaceutical solids.

Fluid bed drying and the process behaviour of the pharmaceutical solids were monitored by the pressure difference over the bed. The approach is advantageous for the studies made in precisely controlled and monitored fluid beds.

The developed multichamber microscale fluid bed with the process control and monitoring solutions is a promising tool for the preformulation and process optimisation studies of the pharmaceutical solids. The fundamental advantages could be achieved with expensive and scarce drug molecules since the same set-up can be used for the several studies.

REFERENCES

Aldridge, P., Evans, C., Ward, H., Colgan, S., Boyer, N. and Gemperline, P., 1996. Near-IR detection of polymorphism and process-related substances. *Anal. Chem.* **68** 997-1002.

Ali, F.S., Inculet, I.I., Tedoldi, A., 1999. Charging of polymer powder inside a metallic fluidized bed. *J. Electrostat.* **45** 199-211.

Alkan, M.H., Groves, M.J., Roland, C.L., Teng, C.D., Dwyer, E.M. and Patel, M.C., 1988. Small-scale film coating of tablets, pellets, and granules. *Pharm. Technol.* **12** (6) 98-104.

Ando, H., Ishii, M., Kayno, M. and Ozawa, H., 1992. Effect of moisture on crystallization of theophylline in tablets. Drug Dev. Ind. Pharm. **18** 453-467.

Andersson, M., Folestad, S., Gottfries, J., Johansson, M., Josefson, M. and Wahlund, K.-G., 2000. Quantitative analysis of film coating process by in-line NIR spectrometry and multivariate batch calibration. *Anal. Chem.* **72** 2099-2108.

Bailey, A.G., 1984. Electrostatic phenomena during powder handling. *Powder Technol.* **37** 71-85.

Bailey, A.G., 1993. Charging of solids and powders. *J. Electrostat.* **30** 167-180.

Berntsson, O., Zackrisson, G. and Östling G., 1997. Determination of moisture in hard gelatin capsules using near-infrared spectroscopy: applications to at-line process control of pharmaceutics. *J. Pharm. Biomed. Anal.* **15** 895-900.

Bjerrum, O. J., 2002. New safe medicines faster: a proposition for a pan-European research effort. *Nature Reviews Drug Discovery* 1(5) 395-398.

Blair, T.C., Buckton, G., Beezer, A.E. and Bloomfield, S.F., 1990. The interaction of various types of microcrystalline cellulose and starch with water. *Int. J. Pharm.* **63**(3) 251-257.

Blanco, M., Coello, J., Iturriaga, H., Maspoch, S. and de la Pezuela, C., 1998. Near-infrared spectroscopy in pharmaceutical industry. *Analyst* **123** 135R-150R.

Bock, T.K. and Kraas, U., 2001. Experience with the Diosna mini-granulator and assessment of process scalability. *Eur. J. Pharm. Biopharm.* 52 297-303.

Bogardus, J.B., 1983. Crystalline anhydrous-hydrate phase changes of caffeine and theophylline in solvent-water mixtures. *J. Pharm. Sci.* **72** 837-838.

Brittain, H.G., Bogdanowich, S.J., Bugay, D.E., DeVincentis, J., Lewen, G. and Newman, A.W., 1991. Physical characterization of pharmaceutical solids. *Pharm. Res.* **8**(8) 963-973.

Browne, H.J. and Olsson, K.I., 1998. Discussion of control systems in pharmaceutical manufacturing. *Pharm. Eng.* **18** (4) 84-92.

Buice, R., Gold, T., Lodder, R. and Digenis, G., 1995. Determination of moisture in intact gelatin capsules by near-infrared spectroscopy. *Pharm. Res.* **12** 161-163.

Buckton, G., Yonemochi, E., Hammond, J. and Moffat, A., 1998. The use of near infra-red spectroscopy to detect changes in the form of amorphous and crystalline lactose. *Int. J. Pharm.* **168** 231-241.

Buckton, G., Yonemochi, E., Yoon, W.L. and Moffat, A., 1999. Water sorption and near IR spectroscopy to study the differences between microcrystalline cellulose and silicified microcrystalline cellulose before and after wet granulation. *Int. J. Pharm.* **181** 41-47.

Buijs, K. and Choppin, G.R., 1963. Near-infrared studies of the structure of water. I. Pure Water. *J. Chem..Phys.* **39** 2035-2041.

Byrn, S.R., Pfeiffer, R.R. and Stowell, J.G., 1999. Solid-state chemistry of drugs. 2nd ed., West Lafayette: SSCI Inc.

Byrn, S.R., Pfeiffer, R., Ganey, M., Hoiberg, C. and Poochikian, G., 1995. Pharmaceutical solids: a strategic approach to regulatory considerations. *Pharm. Res.* **12** (7) 945-954.

Callis, J., Illman, D. and Kowalski, B., 1987. Process analytical chemistry. *Anal. Chem.* **59** 624A-637A.

Carter, P.A., Cassidy, O.E., Rowley, G., Merrifield D.R., 1998. Triboelectrification fractionated crystalline and spray-dried lactose. *Pharm. Pharmacol. Commun.* **4** 111-115.

Chitester, D.C., Kornosky, R.M., Fan, L.-S. and Danko, J.P., 1984. Characteristics of fluidization at high pressure. *Chem. Eng. Sci.* **39** 253-261.

Ciborowski, J., Wlodarski, A., 1962. On electrostatic effects in fluidized beds. *Chem. Eng. Sci.* **17** 23-32.

Ciurczak, E.W., Torlini, R.P. and Demkowicz, M.P., 1986. Determination of particle size of pharmaceutical raw materials using near-infrared reflectance spectroscopy. *Spectroscopy* **1** 36-39.

Cross, J.A., 1987. Electrostatic: Principles, problems and Applications. IOP Publishing ltd., Bristol, UK.

Curcio, J.A. and Petty, C.C., 1951. The near infrared absorption spectrum of liquid water. *J. Optic. Soc. Am.* **41** 302-304.

Davidson, J.F., Clift, R. and Harrison, D., 1985. Fluidization. 2nd ed., Academic Press, Orlando, Florida, USA.

Delwiche, S., Pitt, R. and Norris, K., 1991. Examination of starch-water and cellulose-water interactions with near infrared (NIR) diffuse reflectance spectroscopy. *Starch/Stärke* **43** 415-422.

Derksen, M.W.J., van de Oetelaar, P.J.M. and Maris, F.A., 1998. The use of near-infrared spectroscopy in the efficient prediction of the residual moisture of a freeze-dried product. *J. Pharm. Biomed. Anal.* **17** 473-480.

Dreassi, E., Ceramelli, G., Corti, P., Perruccio, P. and Lonardi, S., 1996. Application of near-infrared reflectance spectrometry to the analytical control of pharmaceuticals: ranitidine hydrochloride tablet production. *Analyst* **121** 219-222.

Drennen, J.K. and Lodder R.A., 1990. Nondestructive near-infrared analysis of intact tablets for determination of degradation products. *J. Pharm. Sci.* 79 (7) 622-627.

Duddu, S.P., Das, N.G., Kelly, T.P. and Sokoloski, T.D., 1995. Microcalorimetric investigation of phase transitions: I. Is water desorption from theophylline · HOH a single-step process?. *Int. J. Pharm.* **114** 247-256.

Dyrby, M., Engelsen, S.B., Nørgaard, L., Bruhn, M. And Lundsberg-Nielsen, L., 2002. Chemometric quantitation of the active substance (containing C≡N) in a pharmaceutical tablet using near-infrared (NIR) transmittance and NIR FT-Raman spectra. *Appl. Spectrosc.* **56** (5) 579-585.

Eilbeck, J., Rowley, G, Carter, P.A. and Fletcher, E.J., 1999. The effect of materials of construction of pharmaceutical processing equipment and drug delivery devices on the triboelectrification of size fractionated lactose. *Pharm. Pharmacol. Commun.* **5** 429-433.

Eilbeck, J., Rowley, G., Carter, P.A. and Fletcher, E.J., 2000. Effect of contamination of pharmaceutical equipment on powder triboelectrification. *Int. J. Pharm.* **195** 7-11.

Ergun, S., 1952. Fluid flow through packed columns. *Chem. Eng. Progr.* **48** 89-94.

Fielden, K., Newton, J., O'Brien, P. and Rowe, R., 1988. Thermal studies on the interaction of water and microcrystalline cellulose. *J. Pharm. Pharmacol.* **40** 674-678.

Fodor, I., Forgács, A. and Berta, I., 1991. Static control of charge decay in industry - hazard and risk. *Inst. Phys. Conf. Ser.* **118** (4) 191-196.

Fornes, V. and Chaussidon, J., 1978. An interpretation of the evolution with temperature of the v_2+v_3 combination band in water. *J. Chem. Phys.* **68** 4667-4671.

Frake, P., Greenhalgh, D., Grierson, S.M., Hempenstall, J.M. and Rudd, D.R., 1997. Process control and end-point determination of a fluid bed granulation by application of near infra-red spectroscopy. *Int. J. Pharm.* 151 75-80.

Frake, P., Gill, I., Luscombe, C.N., Rudd, D.R., Waterhouse, J. and Jayasooriya, U.A., 1998. Near-infrared mass median particle size determination of lactose monohydrate, evaluating several chemometric approaches. *Analyst* **123** 2043-2046.

Froix, M.F. and Nelson, R., 1975. Interaction of water with cellulose from nuclear magnetic resonance relaxation times. Macromol. **8**(6) 726-730.

Fujino, M., Ogata, S. and Shinohara, H., 1985. The electric potential distribution profile in a naturally charged fluidized bed and its effects. *Int. Chem. Eng.* **25**(1) 149-159.

Gaines, C.S. and Windham, W.R., 1998. Effect of wheat moisture content on meal apparent particle size and hardness scores determined by near-infrared reflectance spectroscopy. *Cereal Chem.* **75** 386-391.

Geldart, D., 1973. Types of gas fluidization. *Powder Technol.* **7** 285-292.

Geldart, D., Harnby, N., Wong, A.C., 1984. Fluidization of cohesive powders. *Powder Technol.* **37** 25-37.

Grant, D.J.W., 1999. Theory and origin of polymorphism. In *Polymorphism in pharmaceutical solids*. Brittain, H.G. (Ed.), Marcel Dekker Inc., New York, p. 1-33.

Goebel, S.G. and Steffens, K.-J., 1998. Online-messung der Produktfeuchte und Korngröße in der Wirbelschnicht mit der Nah-Infrarot-Spektroskopie. *Pharm. Ind.* **60** 889-895.

Gottfries, J., Depui, H., Fransson, M., Jongeneelen, M., Josefson, M., Langkilde, F.W. and Witte, D.T., 1993. Vibrational spectrometry for the assessment of active substance in metoprolol tablets: a comparison between transmission and diffuse reflectance near-infrared spectrometry. *J. Pharm. Biomed. Anal.* **14** 1495-1503.

Grosvenor, M.P. and Staniforth, J.N., 1996. The influence of water on electrostatic charge retention and dissipation in pharmaceutical compacts for powders coating. *Pharm. Res.* **13** (11) 1725-1729.

Hailey, P.A., Doherty, P., Tapsell, P., Oliver, T. and Aldridge, P.K., 1996. Automated system for the on-line monitoring of powder blending processes using near-infrared spectroscopy Part I. System development and control. *J. Pharm. Biomed. Anal.* **14** 551-559.

Haleblian, J.K. and McCrone, W.C., 1969. Pharmaceutical applications of polymorphism. *J. Pharm. Sci.* **58** 911-929.

Han, S.M. and Faulkner, P.G., 1996. Determination of SB 216469-S during tablet production using near-infrared reflectance spectroscopy. *J. Pharm. Biomed. Anal.* **14**, 1681-1689.

Hancock, B.C., Clas, S.-D. and Christensen, K 2000. Micro-scale measurement of the mechanical properties of compressed pharmaceutical powders. 2: The elasticity and fracture behavior of microcrystalline cellulose. *Int. J. Pharm.* **209** 27-35.

Harper, W.R., 1967. Contact and frictional electrification. Oxford University Press, London, U.K.

Hassel, D. and Bowman, E., 1998. Process analytical chemistry for spectroscopists. *Appl. Spectrosc.* **52** 18A-29A.

Hearn, G., 1998. Static electricity: concern in the pharmaceutical industry?. *PSTT* **1**(7) 286-287.

Herman, J., Remon, J.P., Visavarungroj, N., Schwartz, J.B. and Klinger, G.H., 1988. Formation of theophylline monohydrate during the pelletisation of microcrystalline cellulose–anhydrous theophylline blends. *Int. J. Pharm.* 42 15-18.

Hicks, M.B., Zhou, G.X., Lieberman, D.R., Antonucci, V., Ge, Z., Shi, Y.-J., Cameron, M. and Lynch, J.E., 2003. *In situ* moisture determination of a cytotoxic compound during process optimisation. *J. Pharm. Sci.* **92** (3) 529-535.

Ilari, J.L., Martens, H. and Isaksson, T., 1988. Determination of particle size in powders by scatter correction in diffuse near-infrared reflectance. *Appl. Spectrosc.* **42** 722-728.

Iwamoto, M., Uozumi, J. and Nishinari, K., 1987. Preliminary investigation of the state of water in foods by near infrared spectroscopy. Budapest: *Int. NIR/NIT Conference*, p 3-12.

Jones, J.A., Last, I.R., Macdonald, B.F. and Prebble, K.A., 1993. Development and transferability of near-infrared methods for determination of moisture in a freeze-dried injection product. *J. Pharm. Biomed. Anal.* **11** (11/12), 1227-1231.

Jørgensen, A., Rantanen, J., Karjalainen, M., Khriachtchev, L., Räsänen, E. and Yliruusi, J., 2002. Hydrate formation during wet granulation studied by spectroscopic methods and multivariate analysis. *Pharm. Res.* **19** 1282-1288.

Kamat, M.S., Lodder, R.A. and DeLuca, P.P., 1989. Near-infrared spectroscopic determination of residual moisture in lyophilized sucrose through intact glass vials. *Pharm. Res.* **6** 961-965.

Kirsch, J.D. and Drennen, J.K., 1996. Near-infrared spectroscopic monitoring of the film coating process. *Pharm. Res.* **13** (2) 234-237.

Kiselnikov, V.N., Vyalkov, V.V. and Filatov, V.M., 1967. On the problem of electrostatic phenomena in a fluidized bed. *Int. Chem. Eng.* **7**(3) 428-431.

Kunii, D. and Levenspiel, O., 1991. Fluidization engineering. 2nd ed., Butterworth-Heinemann, Stoneham, USA.

Laasonen, M., Harmia-Pulkkinen, T., Simard, C., Räsänen, M. and Vuorela, H., 2003. Development and validation of a near-infrared method for the quantitation of caffeine in intact single tablets. *Anal. Chem.* **75** 754-760.

Last, I.R. and Prebble, K.A., 1993. Suitability of near-infrared methods for the determination of moisture in a freeze-dried injection product containing different amounts of the active ingredient. *J. Pharm. Biomed. Anal.* **11** (11/12) 1071-1076.

Lippens, B.C. and Mulder, J., 1993. Prediction of the minimum fluidization velocity. *Powder Technol.* **75** 67-78.

List, K. and Steffens, K.-J., 1996. Überwachung und Steuerung von Granulationsprozessen mit Hilfe der Nah-Infrarot-Spektroskopie. *Pharm. Ind.* **58** 347-353.

Luck, W.A.P., 1976. Hydrogen bonds in liquid water. In *The hydrogen bond.* Schuster, P., Zundel, G. and Sandorfy, C. (Eds.), North Holland Publishing Co, Amsterdam, Holland, p. 1369-1423.

Luner, P., Majuru, S., Seyer, J. and Kemper, M., 2000. Quantifying crystalline form composition in binary powder mixtures using near-infrared reflectance spectroscopy. *Pharm. Dev. Technol.* **5** 231-246.

Luukkonen, P., Rantanen, J., Mäkelä, K., Räsänen, E., Tenhunen, J. and Yliruusi, J.,2001. Characterization of wet massing behavior of silicified microcrystalline cellulose and α-lactose monohydrate using near-infrared spectroscopy. *Pharm. Dev. Technol.* **6**(1), 1-9.

Mackin, L.A., Rowley, G., Fletcher, E.J. and Marriott, R., 1993. An investigation of the role of moisture on the charging tendencies of pharmaceutical excipients. *Proceedings of the 12th Pharmaceutical Technical Conference* **2** 300-317.

Mackin, L., Zanon, R., Park, J.M., Foster, K., Opalenik, H. and Demonte, M., 2002. Quantification of low levels (<10%) of amorphous content in micronised active batches using dynamic vapour sorption and isothermal microcalorimetry. *Int. J. Pharm.* **231** 227-236.

Madan, T. and Kakkar, A.P., 1994. Preparation and characterization of ranitidine-HCl crystals. *Drug. Dev. Ind. Pharm.* **20** 1571-1588.

Maeda, H., Ozaki, Y., Tanaka, M., Hayashi, N. and Kojima, T., 1995. Near infrared spectroscopy and chemometrics studies of temperature-dependent spectral variations of water: relationship between spectral changes and hydrogen bonds. *J. Near Infrared Spectrosc.* **3** 191-201.

Miwa, A., Yajima, T. and Itai, S., 2000. Prediction of suitable amount of water addition for wet granulation. *Int. J. Pharm.* **195** 81-92.

Morris, K.R., Newman, A.W., Bugay, D.E., Ranadive, SA., Singh, A.K., Szyper, M., Varia, S.A., Brittain, H.G. and Serajuddin, A.T.M., 1994. Characterization of humidity-dependent changes in crystal properties of a new HMG-CoA reductase inhibitor in support of its dosage form development. *Int. J. Pharm.* **108** 195-206.

Morris, K.R., Nail, S.L., Peck, G.E., Byrn S.R., Griesser, U.J., Stowell, J.G., Hwang S.-J. and Park, K., 1998. Advances in pharmaceutical materials and processing. *PSTT.* **1** (6) 235-245.

Morris, K., Stowell, J., Byrn, S., Placette, A., Davis, T. and Peck, G., 2000. Accelerated fluid bed drying using NIR monitoring and phenomenological modeling. *Drug Dev. Ind. Pharm.* **26** 985-988.

Morris, K.R., Griesser, U.J., Eckhardt, C.J. and Stowell, J.G., 2001. Theoretical approaches to physical transformations of active pharmaceutical ingredients during manufacturing process. *Adv. Drug. Deliv. Rew.* **48** 91-114.

Murtomaa, M., Ojanen, K. and Laine, E., 2002a. Effect of surface coverage of a glass pipe by small particles on the triboelectrification of glucose powder. *J. Electrostat.* **54** 311-320.

Murtomaa, M., Harjunen, P., Mellin, V., Lehto, V.-P. and Laine, E., 2002b. Effect of amorphicity on the triboelectrification of lactose powder. *J. Electrostat.* **56** 103-110.

Nguyen, N.-A.T., Ghosh, S., Gatlin, L.A. and Grant, D.J.W., 1994. Physicochemical characterization of the various solid forms of carbovir, an antiviral nucleoside. *J. Pharm. Sci.* **83** 1116-1123.

Noda, K., Uchida, T., Makino, T. and Kamo, H., 1986. Minimum fluidization velocity of binary mixture of particles with large size ratio. *Powder Technol.* **46** 149-154.

Norris, K. and Williams, P., 1983. Optimization of mathematical treatment of raw near-infrared signal in the measurement of protein in hard red spring wheat. I. Influence of particle size. *Cereal Chem.* **61** 158-165.

O'Neil, A., Jee, R. and Moffat, A., 1998. The application of multiple linear regression to the measurement of the median particle size of drugs and pharmaceutical excipients by near-infrared spectroscopy. *Analyst* **123** 2297-2302.

O'Neil, A., Jee, R. and Moffat, A., 1999. Measurement of cumulative particle size distribution of microcrystalline cellulose using near infrared reflectance spectroscopy. *Analyst* **124** 33-36.

Osborne, B.G., Fearn, T. and Hindle, P.H., 1993. In *Practical NIR Spectroscopy with Applications in Food and Beverage Industry Analysis*. 2nd ed., Longman, Harlow, UK.

Otsuka, M. and Kaneniwa, N., 1990. Effect of grinding on the crystallinity and chemical stability in the solid state of cephalothin sodium. *Int. J. Pharm.* **62** 65-73.

Otsuka, M., Kaneniwa, N., Otsuka, K., Kawakami, K., Umezawa, O. and Matsuda, Y., 1992. Effect of geometric factors on hydration kinetics of theophylline anhydrate tablets. *J. Pharm. Sci.* **81** 1189-1193.

Phadnis, N.V. and Suryanarayanan, R., 1997. Polymorphism in anhydrous theophylline-implications on the dissolution rate of theophylline tablets. *J. Pharm. Sci.* **86** 1256-1263.

Pimental, G.C. and McClellan, A.L., 1960. In *The Hydrogen Bond.* W.H. Freeman, San Francisco, U.S.A.

Plugge, W. and van der Vlies, C., 1996. Near-infrared as a tool to improve quality. *J. Pharm. Biomed. Anal.* **14** 891-898.

Rantanen, J. and Yliruusi J., 1998. Determination of particle size in a fluidized bed granulator with a near infrared set-up. *Pharm. Pharmacol. Commun.* **4** 73-75.

Rantanen, J., Lehtola, S., Rämet, P., Mannermaa, J.-P. and Yliruusi, J., 1998. On-line monitoring of moisture content in an instrumented fluidized bed granulator with a multi-channel NIR moisture sensor. *Powder Technol.* **99** 163-170.

Rantanen, J., Antikainen, O., Mannermaa, J.-P. and Yliruusi, J., 2000a. Use of the near-infrared reflectance method for measurement of moisture content during granulation. *Pharm. Dev. Technol.* **5**(2) 209-217.

Rantanen, J., Känsäkoski, M., Suhonen, J., Tenhunen, J., Lehtonen, S., Rajalahti, T., Mannermaa, J.-P. and Yliruusi, J., 2000b. Next generation fluidized bed granulator automation. *AAPS PharmSciTech.* **1**: article 10.

Rantanen, J., Räsänen, E., Antikainen, O., Mannermaa, J.-P. and Yliruusi, J., 2001a. In-line moisture measurement during granulation with a four wavelength near infrared sensor: an evaluation of process-related variables and a development of non-linear calibration model. *Chem. Int. Lab. Syst.* **56** 51-58.

Rantanen, J.T., Laine, S.J., Antikainen, O.K., Mannermaa, J.-P., Simula, O.E. and Yliruusi, J.K., 2001b. Visualization of fluid-bed granulation with self-organizing maps. *J. Pharm. Biomed. Anal.* **24** 343-352.

Rao, T.R. and Bheemarasetti, J.V. Ram, 2001. Minimum fluidization velocities of mixtures of biomass and sands. *Energy* **26** 633-644.

Roston, D.A., Walters, M.C., Rhinebarger, R. and Ferro, L.J., 1993. Characterization of polymorphs of a new anti-inflammatory drug. *J. Pharm. Biomed. Anal.* **4/5** 293-300.

Rowe, R.C., 2000. Small is beautiful. *PSTT* **3** 187-188.

Ruotsalainen, M., Heinämäki, J., Rantanen, J. and Yliruusi. J., 2002. Development of an automation system for a tablet coater. *AAPS PharmSciTech* **3**: article 14.

Saxena, S.C. and Vogel, G.J., 1977. The measurement of incipient fluidization velocities in a bed of coarse dolomite at temperature and pressure. *Trans. Inst. Chem. Eng.* **55** 184-189.

Sekulic, S.S., Ward, H.W., Brannegan, D.R., Stanley, E.D., Evans, C.L., Sciavolino, S.T., Hailey, P.A. and Aldridge, P.K., 1996. On-line monitoring of powder blend homogeneity by near-infrared spectroscopy. *Anal.Chem.* **68** 509-513.

Seyer, J., Luner, P. and Kemper, M., 2000. Application of diffuse reflectance near-infrared spectroscopy for determination of crystallinity. *J. Pharm. Sci.* **89** 1305-1316.

Shefter, E. and Higuchi, T., 1963. Dissolution behavior of crystalline solvated and nonsolvated forms of some pharmaceuticals. *J. Pharm. Sci.* **52** 781-791.

Sinsheimer, J.E. and Poswalk, N.M., 1968. Pharmaceutical applications of the near infrared determination of water. *J. Pharm. Sci.* **57** 2007-2010.

Smith, A., 2001. New safe medicines faster. *Trends Pharmacol. Sci.* **22**(2) 62.

Smith, A., 2002. Screening for drug discovery: The leading question. *Nature* **418** 453-459.

Staniforth, J.N., Cryer, S., Ahmed, H.A. and Davies, S.P., 1989. Aspects of pharmaceutical tribology. *Drug Dev. Ind. Pharm.* **15** 2265-2294.

Staniforth, J.N., 2000. Powder flow, in *Pharmaceutics: the science of dosage form design.* Aulton, M.E. (Ed.), 2nd ed., Churchill Livingstone, London, U.K., p. 600-615.

Stein, H.H. and Ambrose, J.M., 1963. Near-infrared method for determination of water in aluminium aspirin. *Anal. Chem.* **35** (4) 550-552.

Suihko, E., Ketolainen, J., Poso, A., Ahlgren, M., Gynther, J. and Paronen, P., 1997. Dehydration of theophylline monohydrate-a two step process. *Int. J. Pharm.* **158** 47-55.

Sun, C., Zhou, D., Grant, D.J.W. and Young Jr, V.G., 2002. Theophylline monohydrate. *Acta Cryst* **E58** o368-o370.

Suzuki, E., Shimomura, K. and Sekiguchi, K., 1989. Thermochemical study of theophylline and its hydrate. *Chem. Pharm. Bull.* **37** 493-497.

Taylor, L.S. and York, P., 1998a. Characterization of the phase transitions of trehalose dihydrate on heating and subsequent dehydration. *J. Pharm. Sci.* **87** 347-355.

Taylor, L.S. and York, P., 1998b. Effect of particle size and temperature on the dehydration kinetics of trehalose dihydrate. *Int. J. Pharm.* **167** 215-221.

Visser, J., 1989. Van der Waals and other cohesive forces affecting powder fluidization. *Powder Technol.* **58** 1-10.

Watano, S., Terashita, K. and Miyanami, K., 1990. Development and application of infrared moisture sensor to complex granulation. *Bull. Univ. Osaka. Pref., Series A*, **39** 187-197.

Watano, S., 1995. *Mechanism and control of granule growth in fluidized bed granulation.* Ph.D. Thesis, Collage of Engineering, University of Osaka, Japan.

Watano, S., Takashima, H., Sato, Y., Yasutomo, T. and Miyanami, K., 1996a. Measurement of moisture content by IR sensor in fluidized bed granulation. Effects of operating variables on the relationship between granule moisture content and absorbance IR spectra. *Chem. Pharm. Bull.* **44** 1267-1269.

Watano, S., Takashima, H., Sato, Y., Miyanami, K. and Yasutomo, T., 1996b. IR absorption characteristics of an IR moisture sensor and mechanism of water transfer in fluidized bed granulation. *Advanced Powder Technol.* **7** 279-289.

Watano, S., Suzuki, T., Taira, T. and Miyanami, K., 1998. Continuous monitoring and mechanism of electrostatic charge of powder in fluidized bed process. *Chem. Pharm. Bull.* **46**(9) 1438-1443.

Wen, C.Y. and Yu Y.H., 1966. A generalized method for predicting the minimum fluidization velocity. *AIChE J.* **12**(3) 610-612.

White, J., 1994. On-line moisture detection for a microwave vacuum dryer. *Pharm. Res.* **11** 728-732.

Williams, P. and Norris, K. (Eds.), 1987. *Near-infrared technology in the agricultural and food industries.* 1st ed., American Association of Cereal Chemists, Inc., St. Paul (MI), USA.

Vladykina, T.N., Deryagin, B.V. and Toporov, Y.P., 1985. The effect of surface roughness on triboelectrification of insulators. *Phys. Chem. Mech. Surfaces* **3** 2817-2821.

Workman, J., Jr., 1993. A review of process near infrared spectroscopy: 1980-1994. *J. Near Infrared Spectrosc.* **1** 221-245.

Workman, J.J., Jr., 1999. Review of process and non-invasive near infrared and infrared spectroscopy: 1993-1999. *Appl. Spectrosc. Reviews* **34** (1&2) 1-89.

Yu, L., Reutzel, S.M. and Stephenson G.A., 1998. Physical characterization of polymorphic drugs: an integrated characterization strategy. *PSTT.* **1** (3) 118-127.

Yang, W.-C., 1999. Fluidization solids handling and processing. Noyes Publications, Westwood, New Jersey, USA.

Zhu, H., Yuen, C. and Grant, D.J.W., 1996. Influence of water activity in organic solvent + water mixtures on the nature of the crystallizing drug phase. 1. Theophylline. *Int. J. Pharm.* **135** 151-160.

Zografi, G., Kontny, M.J., Yang, A.Y.S. and Brenner, G.S., 1984. Surface area and water vapor sorption of microcrystalline cellulose. *Int. J. Pharm.* **18**(1-2) 99-116.

Zografi, G., 1988. States of water associated with solids. *Drug. Dev. Ind. Pharm.* **14** 1905-1926.